JOURNAL OF CATALYSIS **161,** 839–860 (1996)
ARTICLE NO. 0247

Promotion Effects of Titanium on Partial Oxidation of Methanol over Vanadium Pentoxide Catalysts

Laura Briand,[1] Luis Gambaro, and Horacio Thomas

Centro de Investigación y Desarrollo en Procesos Catalíticos (CINDECA), Universidad Nacional de la Plata, (1900) La Plata, Buenos Aires, Argentina

Received November 21, 1994; revised September 29, 1995; accepted January 19, 1996

This article reports studies on the catalytic activity of V_2O_5 coprecipitated with different TiO_2 concentrations, and on the chemical characterization of the fresh and used catalysts by the following methods of chemical analyses: EDAX, XRD, FTIR, SEM, BET, TPR, and XPS. Catalytic tests were performed under integral and differential conditions. In the former (integral) series of experiments, formaldehyde, methyl formate, methylal, and CO were obtained as major products of methanol partial oxidation. A minor production of CO_2 and dimethyl ether was noticed as well. Under the latter (differential) conditions, the results led to the notion of catalytic activity (reaction rate) dependence on the surface concentration of vanadium. From calculation of the turnover frequencies, it was concluded that both the catalytic activity and the HCHO production decrease with stronger V=O bonds. In turn, the reactivity of those species was influenced by addition of TiO_2.

INTRODUCTION

It is a well known fact that vanadium–titanium catalysts, both mass and supported, are used in industry for the partial oxidation of hydrocarbons and for the selective catalytic reduction (SCR) of NO with NH_3. In spite of many papers dealing with this system, few data are available about the real nature of the active phase after a long catalytic test period. Most authors correlate the catalytic activity, reached after a short reaction periods (hours), to the characterization of the fresh catalysts. On the other hand, the literature shows extensive studies of the catalytic effect of a large number of supports. The catalytic behavior of the V oxide is considerably influenced by the specific nature of the oxide support and by the degree of coverage of the support. Moreover, contrasting opinions on the surface structure of supported V oxide and its reactivity can be found in the literature (1).

Some authors have suggested that the activity of supported vanadium depends on the selective exposure of the plane (001) of V_2O_5, where the maximum concentration of V=O bond surface sites is found. In turn, some others, depending on the nature of the oxide support, have proposed the presence of either mono- or polymeric V oxide species. The last group of authors have suggested the formation of a dioxo species on TiO_2, in contrast to the monooxo species usually found in V oxide. More recently, Deo *et al.* (2) used the partial oxidation of methanol to analyze the reactivity of the surface vanadium redox sites present in vanadium oxide supported on SiO_2, Al_2O_3, ZrO_2, TiO_2, and Nb_2O_5. By means of spectroscopic analysis, they concluded that, regardless of the type of support, the vanadium was in the form of isolated and polymeric vanadium oxide species. They demonstrated that the catalyst activity to selective oxidation of methanol (under differential reaction conditions), was not related to the V=O strength, but appear to be related to the reducibility of the V–O–Support bond.

In the more recent literature about the structural characteristics of coprecipitated VTiO systems and its activity in selective oxidation reactions, there are some particularly important contributions. Slinkard *et al.* (3) have demonstrated that coprecipitated VTiO catalysts show a high selectivity to the production of acetaldehyde and acetic acid, when *n*-butenes are used as reactant. Phases in the solids were V_2O_5, TiO_2 anatase and rutile, and a solid solution of V^{4+} in TiO_2, the proportions of which had direct influence on the catalytic activity. The more active and selective catalysts for the oxidation of *n*-butenes to acetic acid were those containing a solid solution of V^{4+} in TiO_2 and reduced vanadium oxides. They concluded that the function of TiO_2 in the VTiO catalysts may be to serve as a host for the V^{4+} and to stabilize it against oxidation to the less active V^{5+} state. Moreover, catalysts containing rutile had higher selectivities to acetic acid and acetaldehyde than anatase-containing catalysts. This fact was attributed to the higher concentration of V^{4+} in the rutile lattice, to a different position of V^{4+} in it, and to higher stability of products on rutile than on anatase surfaces.

Fierro *et al.* (4) have characterized a series of coprecipitated V_2O_5–TiO_2 (anatase) catalysts and correlated their physicochemical properties to their catalytic activity in

[1] To whom correspondence should be addressed.

0021-9517/96 $18.00

the selective oxidation of isobutene. They found that the catalytic activity of these preparations depended on the V/(V + Ti) ratio, reaching a maximum at V/(V + Ti) = 0.11. For this catalyst, XPS analysis showed surface enrichment in a vanadium oxide phase, whereas temperature-programmed reduction revealed the lowest temperature for hydrogen reduction. Those catalysts having particularly high vanadium concentrations [V/(V + Ti) ≥ 0.2] showed clear evidence of the presence of tridimensional V_2O_5 crystallites, and as these samples were less active, they deduced that the activity was directly related to a highly dispersed oxidic vanadium phase.

Cavani *et al*. (5) have investigated vanadium–titanium oxide catalysts as prepared by different methods such as flash drying, coprecipitation, wet impregnation, and grafting. The results indicated that in addition to crystalline V_2O_5 (found at coverages higher than the monolayer), three vanadium species were present on the surface of TiO_2 : V^{4+} and V^{5+} species strongly interacting with the titanium surface and a weakly interacting V^{5+} species. The coprecipitated catalysts (maximum concentration = 25% V_2O_5) had a higher concentration of strongly interacting vanadium species than the rest of the preparations, as well as a higher catalytic activity for the selective oxidation of *o*-xylene to phthalic anhydride. However, all catalysts, regardless of the preparation methods used and the vanadium concentrations, had the same selectivity.

Cavani *et al*. (6) have characterized and investigated the activity of VTiO systems as prepared by flash-drying coprecipitation from solutions of V^{4+} and Ti^{4+}. The resultant catalysts were formed by anatase and three different vanadium species: (1) V(IV) in strong interaction with the support (possibly forming a monolayer), (2) V(V), easily reducible to V(IV) and V(III), and strongly interacting with the support, and (3) an amorphous V_2O_5 phase. The analysis of the activity of these systems in the ammoxidation of toluene to benzonitrile and the dehydrogenation of isopropyl alcohol to acetone indicated that the species (1) were the active sites responsible for the toluene activation and the alcohol dehydrogenation and that the species (2) were active in the combustion of ammonia to N_2, while the amorphous phase was inactive.

With regard to the use of coprecipitated VTiO catalysts in the selective oxidation of methanol, we can mention the study of Forzatti *et al*. (7) on V–Ti catalysts with high titanium content. In mass catalysts with V/Ti atomic ratios in the range 0–0.0625, they found that the major products of the methanol partial oxidation were formaldehyde and methyl formate. From a pulse reactor and solids characterization studies, they established that the selectivity towards formate was related to the bifunctional (acid–oxidant) feature of the catalysts, to the surface concentration of vanadium, and to the presence of TiO_2 anatase. They also speculated about the mechanism of reaction.

Sambeth *et al*. (8, 9) studied the adsorption–oxidation of methanol over V_2O_5 and coprecipitated VTiO samples between 100 and 200°C at infinite contact times. From a mass spectroscopy analysis of the composition of the gas phase and a study of the variation of the solids' electrical properties (Hall voltage), they concluded that the adsorption took place first, and was then followed by methanol oxidation to formaldehyde, hemimethylal, methyl formate, methylal, CO_2, and CO, in proportions depending on temperature and contact time. They suggested a reaction mechanism in which methanol first oxidizes to HCHO. This species can undergo desorption, be oxidized to CO, or otherwise condense with other methanol molecule to give hemimethylal. In turn, the adsorbed hemimethylal can either oxidize to methyl formate or condense with other methanol molecule to give rise to methylal.

It is clear that a large number of variants have been adopted in preparation of the coprecipitated VTiO systems. Each of these leads, in turn, to solids of distinct physicochemical characteristics so that more than one catalytically active phase has been proposed. However, little has been studied about the utilization of this system in the selective oxidation of methanol; moreover, there is a lack of information on the modifications undergone by the VTiO catalysts over long periods of reaction with methanol. Because of this, our purpose is to conduct a complete study about the catalytic behavior of a broad series of coprecipitated VTiO solids, their physicochemical properties both before the reaction and after reaching steady state, a situation in which an equilibrated catalyst is obtained. In addition, we present the catalytic activity under differential reaction conditions, as well as experimental evidence supporting a mechanism—previously published by our group (8, 9)—for the reaction of methanol on VTiO catalysts.

EXPERIMENTAL

Synthesis of the Catalysts

Vanadium pentoxide was prepared from a solution of NH_4VO_3 on hydrochloric acid (Merck, PA), which was further neutralized to pH = 6 with concentrated NH_4OH (Merck, P. A.). The precipitate was filtered and washed with water to eliminate the NH_4Cl formed during the neutralization. It was finally dried at 120°C for 12 h and calcined at 500°C in air for 24 h.

We synthesized five samples of V_2O_5–TiO_2 with titanium percentages from 10 to 90%, which were named VT10, VT20, VT50, VT80, and VT90 according to the titanium proportion. All samples were synthesized by mixing $VOCl_3$ and $TiOCl_2$. The $VOCl_3$ was, in turn, prepared just before use, by dissolving NH_4VO_3 (Mallinckrodt AR) in concentrated HCl (Merck P. A.). The $TiOCl_2$ was also prepared just prior to use by hydrolysis of $TiCl_4$ (Carlo Erba RPE).

TABLE 1

Surface and Bulk Analysis of Fresh VTiO Catalysts

	V/V + Ti		% W/W TiO_2 (cell volume Å)		Binding energy (f.w.h.m.), eV			
Sample	Bulk	Surface	Anatase	Rutile	$V(V)_{2p3/2}$	$Ti(IV)_{2p3/2}$	S_{BET} (m^2g^{-1})	Reduction T (°C)
V_2O_5	1.00	1.00	—	—	516.8 (1.9)	—	2.6	311
VT10	0.89	0.82	23 (133.2 ± 0.3)	77 (62.5 ± 0.3)	516.5 (1.6)	457.6 (1.4)	1.6	290
VT20	0.86	0.84	10 (127.8 ± 0.4)	90 (64.8 ± 0.8)	516.6 (1.7)	457.8 (1.4)	2.2	291
VT50	0.56	0.37	90 (135.6 ± 0.2)	10 (62.1 ± 0.2)	516.5 (1.7)	457.8 (1.45)	9.4	343
VT80	0.27	0.38	92 (133.3 ± 0.2)	8 (63.01 ± 0.03)	516.6 (1.8)	458.3 (1.8)	5.3	320
VT90	0.13	0.28	38 (136.66 ± 0.05)	62 (62.52 ± 0.01)	516.7 (1.9)	458.2 (1.75)	4.6	302

These solutions were mixed in the suitable proportions, and adjusted to pH 6 with ammonium hydroxide (Merck P. A.) under constant stirring and cooling. The precipitate was filtered, washed, dried at 120°C, and finally calcined at 500°C in air for 24 h.

All thermal treatments were performed in either quartz or platinum containers, to avoid bronze formation.

Catalyst Characterization

Quantitative analysis. Concentrations of vanadium and titanium of the fresh and used VTiO solids (before and after catalytic reaction, respectively) were determined by means of an Edax Philips 505 microprobe. All samples were homogenized and covered with a very thin layer of gold. The results are listed in Tables 1 and 2.

The maximum relative error in the method is 3% for concentrations higher than $V/(V + Ti) = 0.03$.

BET specific surface. The specific surface of the fresh samples was determined according to the BET method, using Micromeritics Accusorb equipment. The results are shown in Table 1.

X-ray diffraction. X-ray diffraction spectra of the fresh (Fig. 1) and used samples (Table 3) were obtained for 2θ values from 15° to 60° with Philips PW 1390 equipment having Cu$K\alpha$ radiation and a Ni filter. The set of operating conditions utilized was source voltage, 40 kV; source current, 20 mA; goniometer speed, $\Delta(2\theta) = 1°$/min; chart speed, 2 cm/min; slit, 1°/0. 1°/1°. These studies were analyzed according to the ASTM files (10).

The fractions of rutile (X_r) and anatase (X_a) were determined by the equation (11)

$$X_r = (1 + 0.794 I_a/I_r)^{-1}$$

measuring the intensities of the (110) and (101) reflections for rutile (I_r) and anatase (I_a), respectively.

The network parameters were determined by computational calculation of the centroids belonging to the more intense diffraction lines of the anatase and rutile phases. The calculation was based on the average (12)

$$2\theta = \frac{\int 2\theta I(2\theta) d(2\theta)}{\int I(2\theta) d(2\theta)},$$

where

2θ = diffraction angle,
$I(2\theta)$ = diffraction intensity for angle 2θ
d = interplanar distance.

From the centroid, the interplanar distance was calculated by the Bragg law. The network parameters of a crystal, i.e., the dimensions of its unitary cell, can be obtained at several d values if the crystalline system of the substance under

TABLE 2

Surface and Bulk Analysis of Used VTiO Catalysts

	V/V + Ti		% Surface vanadium		% W/W TiO_2 (cell volume Å)		Binding energy (f.w.h.m.), eV		
Sample	Bulk	Surface	V(V)	V(IV)	Anatase	Rutile	$V(V)_{2p3/2}$	$V(IV)_{2p3/2}$	$Ti(IV)_{2p3/2}$
V_2O_5	1.00	1.00	62	38	—	—	516.8	515.4	—
VT10	0.89	1.00	82	18	—	100 (62.20 ± 1 10^{-2})	516.7	515.2	—
VT20	0.95	1.00	78	22	—	100 (61.40 ± 3 10^{-2})	517.0	515.6	—
VT50	0.56	0.57	87	13	89 (135.70 ± 9 10^{-2})	11 (—)	516.9	515.5	458.5 (1.7)
VT80	0.24	0.36	83	17	96 (133.3 ± 0.2)	4 (—)	516.3	515.0	458.3 (1.7)
VT90	0.08	0.51	63	37	38 (133.77 ± 5 10^{-2})	62 (62.17 ± 7 10^{-2})	516.7	515.4	458.3 (1.7)

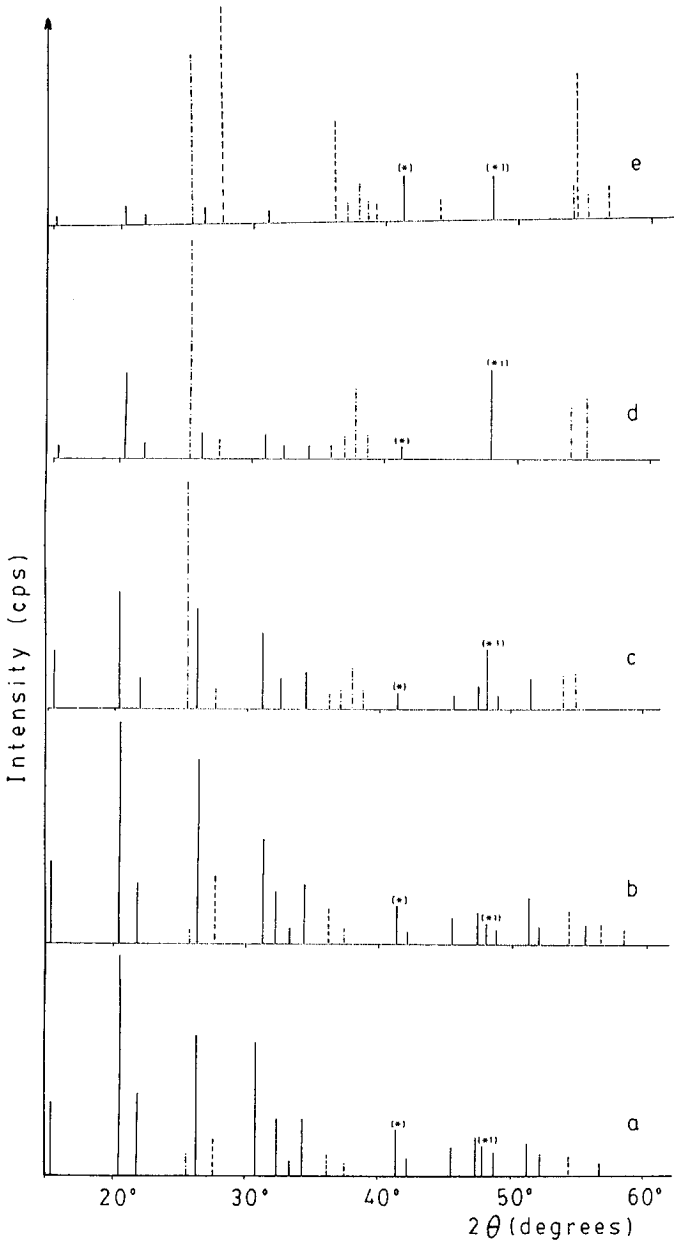

FIG. 1. X-ray diffraction spectra of fresh VTiO samples: (A) VT10, (B) VT20, (C) VT50, (D) VT80, and (E) VT90. Symbols: — V_2O_5; - - - TiO_2 rutile; ------- TiO_2 anatase; (∗) V_2O_5 or rutile and (∗1) V_2O_5 or anatase.

study and the Miller's indices of the corresponding planes are known. Both TiO_2-anatase and TiO_2-rutile crystallize in the tetragonal system ($a_0 = b_0 \neq c_0$ with all right angles) where the relationships between interplanar distances and unitary cell dimensions are

$$d^{-2} = (h^2 + k^2)a_0^{-2} + l^2 c_0^{-2}, \qquad [1]$$

where h, k, l are Miller's indices of the plane under consideration, and a_0, c_0 are networkparameters.

The signals selected for the crystalline network parameters were digitalized by means of the sum of at least four scans, so as to obtain an optimal signal. The scans were made under the same set of operating conditions used before, except that the goniometer speed was lower ($\Delta(2\theta) = 0.01^\circ$/min). Once the limiting angles of peaks were established, the location of the centroids and the interplanary distance d were calculated with the computer program. By using the interplanary distances and the literature values of the hkl indices for every selected plane, we arrived at the parameters a_0, c_0 in a tetragonal system (TiO_2 anatase and rutile) by using Eq. [1]. The uncertainty range (confidence limits) of the parameters were expressed as the relative error between the calculated values of only one scan and those obtained for a minimum of four scans.

Also in all the catalysts we calculated the width at midheight (FWHM) of plane (001) of the V_2O_5 phase ($2\theta = 20.27^\circ$). The signal was digitized using the method described in the previous paragraph, and the value thus obtained was compared to the instrumental width attained with the plane (111) of silicon ($2\theta = 28.44^\circ$), which is considered a crystal of infinite size.

TABLE 3

DRX Analysis of Used VT10 Catalyst

Angle (2θ)	d (Å)	Relative intensity	Phase
15.5	5.71	19	V_2O_5
20.4	4.35	75	V_2O_5
21.8	4.07	20	V_2O_5
26.3	3.38	28	V_2O_5,VO_2(A)
27.0	3.30	8	V_2O_4,V_6O_{13}
27.7	3.22	31	Rutile
27.9	3.19	100	V_2O_4,V_6O_{13}
31.1	2.87	31	V_2O_5,VO_2(B)
32.5	2.75	11	V_2O_5
33.5	2.67	9	V_2O_5,VO_2(A),VO_2(B), V_6O_{13},V_2O_4
34.5	2.60	11	V_2O_5
36.3	2.47	12	VO_2(B),V_6O_{13}, Rutile
37.1	2.42	50	V_2O_5,V_6O_{13},V_2O_4, Anatase
39.9	2.26	5	VO_2(A),VO_2(B), V_6O_{13},V_2O_4
41.5	2.17	12	V_2O_5, Rutile
42.3	2.14	20	V_2O_5,V_2O_4
45.5	1.99	6	V_2O_5,VO_2(A),V_6O_{13}
47.3	1.92	9	V_2O_5,VO_2(A)
51.4	1.78	6	V_2O_5
52.0	1.76	5	V_2O_5,VO_2(B)
54.5	1.68	7	Rutile
55.6	1.65	31	VO_2(A),VO_2(B),V_6O_{13}, V_2O_4, Anatase
57.6	1.60	10	VO_2(A),VO_2(B),V_6O_{13}, V_2O_4

Temperature-programmed reduction (TPR). As a first step of the study, reductions were carried out at temperatures programmed between 100 and 600°C, for all samples, with a conventional equipment. The next step consisted of tests in each of which the reductions were stopped at temperatures corresponding to the thermogram peaks; then the reduced solids were characterized by different spectroscopic techniques (Table 4). The samples were reduced in a gas stream containing 10% of H_2 in N_2, with a total flow of 55 cm^3 min^{-1} and a heating rate of 5°C min^{-1} (13).

Infrared analysis. Samples were analyzed by infrared spectroscopy with Bruker IFS 66 FTIR equipment. Infrared bands were identified according to the data reported by Frederickson *et al.* (14), Fabri *et al.* (15), Theobald (16), and Barraclough (17) with regard to V_2O_5 and their reduced oxides. Figure 3 shows the spectra of the fresh samples and positions of the infrared bands of V=O and V–O–V bonds; in turn, Table 5 shows the analysis of the spectra of the used catalysts.

Scanning electron microscopy (SEM). Both fresh and used samples were analyzed with a Philips SEM 505 electron microscope. The photographs correspond to magnification × 2000.

X-ray photoelectron spectroscopy. The oxidation states and surface concentrations of vanadium and titanium (Tables 1 and 2) were determined with a Shimadzu ESCA 750 Electron Spectrometer attached to a ESCAPAC 760 computer for data acquisition and processing purposes. The equipment had an X-ray a source with a magnesium anode, radiation Mg$K\alpha$ at 1251.6 eV, and a bond energy repeatability of 0.2 eV. The working pressure was 10^{-8} Torr. The bond energy of C_{1s} (284.6 eV) was taken as reference.

Catalytic Reactions

The catalytic analysis of samples was carried out in conventional continuous flow apparatus under integral and differential conditions. The conditions for the integral experiments were as follows: sample weight, 300 mg; reaction temperatures, 100–300°C; bed volume, 0.4 cm^3; flow rate, 30 cm^3 (NTP) min^{-1}, and a composition of the feed gas flow of 10% methanol in air. The differential experiments were conducted at a temperature of 150°C; catalyst weight, 50 mg; composition of the feed gas flow, 10% methanol in air, and variable contact times from 0.14 to 0.74 sec, to keep conversions below 13%.

TABLE 4

Phases Identified by XRD and FTIR in Reduced Samples

Sample	Reduction temperatures (°C) [IR frequency of V=O bond (cm^{-1})]		
	*T*1	*T*2	*T*3
V_2O_5	V_2O_5 [1020]	V_2O_5,VO_2(B) [1016]	V_2O_3
VT10	V_2O_5 [1021]	—	V_2O_5,V_2O_4 [1012]
VT20	V_2O_5 [1020]	—	V_2O_5,V_6O_{13} [1014]
VT50	V_2O_5 [1014]	V_2O_5,V_2O_4, V_6O_{13} [1000] amorphous	VO_2(B),V_2O_4 [1002] amorphous
VT80	V_2O_5 [1032]	V_2O_5,VO_2(B) [1003]	V_2O_5 [1000] scarce
VT90	V_2O_5 [1029]	—	V_6O_{13} [1012]

TABLE 5

Infrared Analysis of the Used VTiO Catalysts

Sample	Frequency (cm^{-1})	Assignment
VT10	1009	V=O
	726	V_2O_4
	530	V_2O_4, Rutile
	476	V_2O_5
	429	VO_2(A)
	420	Networkvibrations
VT20	1021	V_2O_5,V_2O_4
	805	V_2O_4
	576	Anatase
	530	V_2O_4, Rutile
	478	V_2O_5
VT50	1023	V_2O_5
	812	V_2O_5,V_2O_4
	528	Anatase, Rutile
VT80	1030	V_2O_5
	657	TiO_2
	537	VO_2(B), Anatase
VT90	1018	V_2O_5,V_2O_4
	650	TiO_2
	549	VO_2(B), Anatase
	436	VO_2(A)

The products of reaction were identified by mass spectrometry and quantified in a Shimadzu GC 8A gas chromatograph, equipped with two columns and a detector of thermal conductivity. Helium at 30 cm^3 (NTP) min^{-1} was used as carrier gas. Formaldehyde, dimethyl ether, methyl formate, methylal, and CO_2 were analyzed in a 3-m Porapak T column, with a temperature program that first kept it at 130°C for 20 min, and then increased it to 170°C at a rate of 5°C min^{-1}. The carbon monoxide was analyzed at 60°C in a 2-m column containing 5 Å molecular sieves.

The quantitative determination of formic acid was done by acid–base volumetric analysis. To this end, the stream leaving the reactor was bubbled through distilled water and then titrated with a NaOH solution. Controls to determine the acidity arising from the rest of the products were also applied. The accuracy of the analytical methods was demonstrated by the fact that the carbon balance was 100 ± 5%.

The reaction temperatures were varied at random. In all the experiments it was considered that the steady state had

been reached when the variations of both the methanol conversion and selectivity to any given product were less than or equal to 5%. Generally, this state was attained after approximately 50 hours of reaction. To verify that the data for the steady state corresponded to a stable catalyst, we repeated the catalytic test at some of the previously studied temperatures.

To certify the possibility of volatilization in the surface vanadium oxide phase as a consequence of prolonged contact with a methanol–oxygen atmosphere, we carried out a quantitative analysis of vanadium in the used catalysts (2).

Oxygen chemisorption. The active surface area of the used catalysts was measured through oxygen chemisorption using the technique described by Oyama *et al.* to quantify the chemisorption sites of V_2O_5, both pure and supported (18, 19). In the present work, however, some modifications to that technique were introduced to adapt it to our catalytic system. They are justified as follows:

1. In the technique described by Oyama *et al.*, the catalysts are initially reduced in hydrogen at 368°C. In our work the catalysts were activated at 150°C in a methanol/air flow under the differential reaction conditions detailed in the previous section. The procedure ensures the availability for chemisorption of only those sites participating in the reaction conditions, in which to TON will be expressed.

2. Before the determination of the O_2 uptake, the samples were heated in flowing He (the flow rate used was the same as that of the differential conditions) for 1 h to the same temperature as that of chemisorption. The purpose of this stage is to desorb the methanol or any reaction product from the solid surface.

3. The chemisorption experiments were carried out with successive 0.50 ml O_2 pulses (at intervals of about 5 min.) in a flow of He until no variations in the area of the oxygen signal were recorded by the TCD. The difference between the area of the peak at saturation and the area of peaks before saturation was attributed to the irreversible uptake of O_2 by the sample.

Oyama *et al.* carried out the chemisorption experiments at 368°C because they verified that value as the temperature at which the surface adsorption of oxygen takes place without modifying the bulk. In our work, the experiments were executed at 200, 250, and 300°C since previous chemisorption studies (using a volumetric method) had indicated that temperatures higher than 300°C produced oxygen diffusion to the bulk of VTiO solids (20, 21). The subsequent sections will treat these studies in greater detail.

RESULTS

Structural Characterization by XRD

Fresh catalysts. Diffraction diagrams of the fresh catalysts are given for simplicity as a bar graphs in Fig. 1. For each sample, the full width at half maximum (FWHM) of the (001) plane was used in the V_2O_5 phase as a parameter of its crystal size (Fig. 2). The analysis of the diagrams indicates that all samples were composed of orthorhombic V_2O_5 and different proportions of TiO_2 anatase and rutile (Table 1). The FWHM values of the plane (001) in vanadium pentoxide are similar to those of the plane (111) in silicon (0.16°). As previously said, this crystal, in an XRD

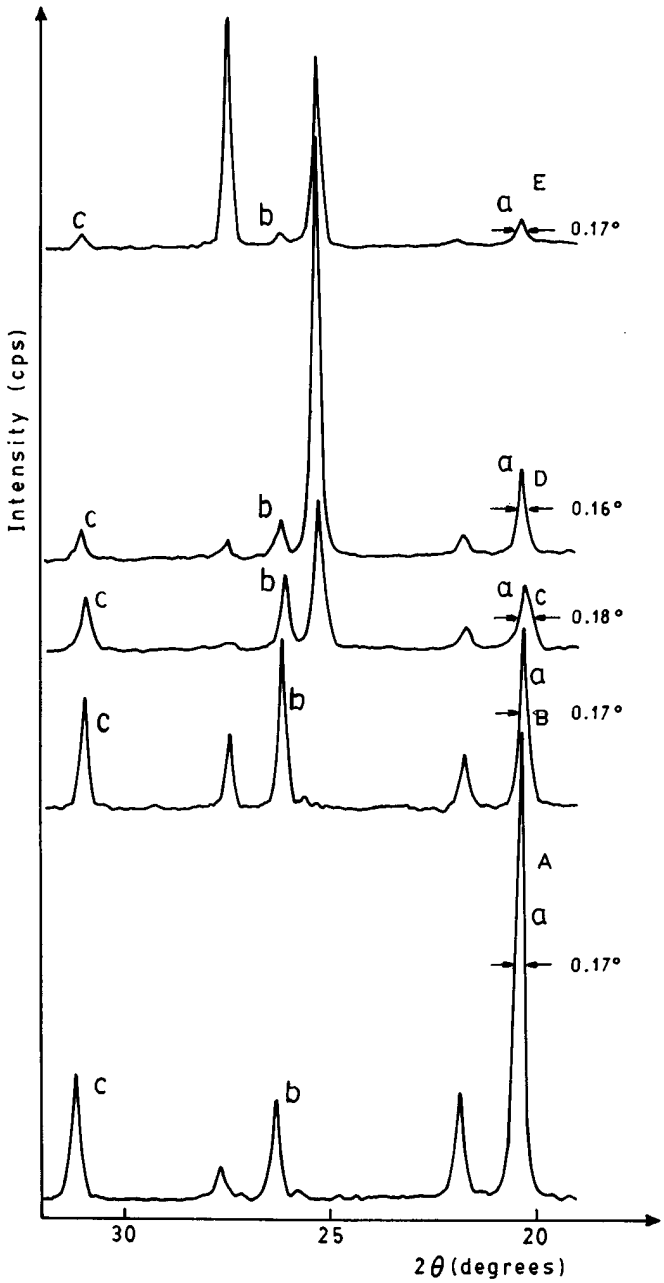

FIG. 2. Comparison of intensities of X-ray reflections (001), (200), and (020) of V_2O_5 phase of samples: (A) VT10, (B) VT20, (C) VT50, (D) VT80, and (E) VT90. Symbols: (a) (001) plane, (b) (200), plane and (c) (020) plane. FWHM of the (001) plane.

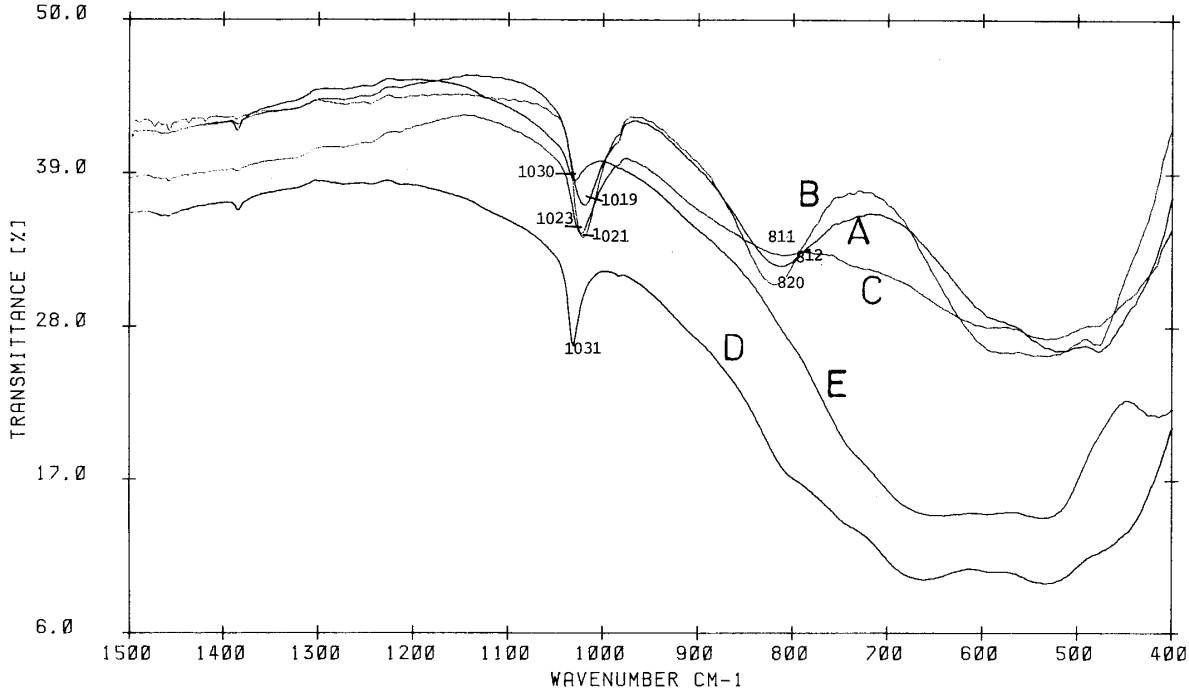

FIG. 3. Infrared spectra of fresh VTiO samples: (A) VT10, (B) VT20, (C) VT50, (D) VT80, and (E) VT90.

analysis, is considered of infinite size. This means, regardless of the V/(V + Ti) ratio, that in all fresh catalysts at least part of the vanadium phase crystallizes in large particles.

As it can be observed in Table 1, the cell volumes of the TiO_2-anatase phase of the fresh VTiO solids are smaller than those of pure anatase (140.7 ± 1.0 Å^3) (the latter was prepared by precipitation in alkaline medium by using $TiCl_4$, dried and calcined in the same way as the catalysts). This cell "shrinkage" is caused by substitution of a titanium atom by a vanadium atom, thus leading to a substitutional solid solution. In TiO_2-rutile cells, we observed an increase of volume with respect to that of the rutile (62.51 ± 5 10^{-2} Å^3) (the latter was prepared by calcination of anatase at 1000°C) for samples VT20 and VT80 and a decrease in sample VT50. No volume variation was detected for the VT90 sample, whereas in the sample VT10 we were not able to detect variations owing to the high measurement error.

Used catalysts. According to XRD and FTIR analysis, the used V_2O_5 consisted of reduced vanadium oxides V_2O_4,VO_2(A), and in a small amount, also V_2O_5 (IR signal at 968 cm^{-1}). Phases V_6O_{13} and monoclinic VO_2(B) might also be present, but this cannot be definitely established since their signals overlap themselves (10). As shown by the XRD analysis of used catalysts VT10 (Table 3), some signals exhibited by the used samples were difficult to identify, because the reduced vanadium oxides (V_2O_4,V_6O_{13},VO_2(A), and VO_2(B)) have coincidental diffraction lines (10). Therefore, a comparative analysis of the oxides identified by FTIR and DRX was conducted to determined those titanium and vanadium phases actually present in the samples. The used catalysts, i.e.,VT10 and VT20, exhibited mainly V_2O_5,V_2O_4, and TiO_2 rutile. In the used VT50 and VT80 samples, the major phases were TiO_2 anatase and V_2O_5, though small signals of the V_2O_4 phase in VT80, and of VO_2(B) in the VT50 sample, were also observed. In the used VT90 catalyst, the signals exhibited were mostly of anatase and rutile, through small signals, which were thought to correspond to the V_2O_4 phase, were also observed.

In those catalysts that allowed the network parameters to be calculated, we observed an important cell volume shrinkage in the phases anatase and rutile. This result is not surprising, since it is reasonable that the reduction of V(V) to V(IV) during the reaction favors the formation of a solid solution.

Structural Characterization by FTIR

Fresh catalysts. The FTIR analysis showed two bands corresponding to the vanadium phase: double bond, V=O, at approximately 1020 cm^{-1}, and the V–O–V bond, at 820 cm^{-1}. The broad band between 470 and 600 cm^{-1} corresponds, in turn, to network vibrations of vanadium and titanium phases (Fig. 3). Therefore, an increase of titanium content causes a shift in the vanadyl band to higher frequencies.

Used catalysts. The signal found at 1002 cm^{-1} in the infrared spectrum of the used V_2O_5 corresponds to species with a high proportion of reduced vanadium–oxygen

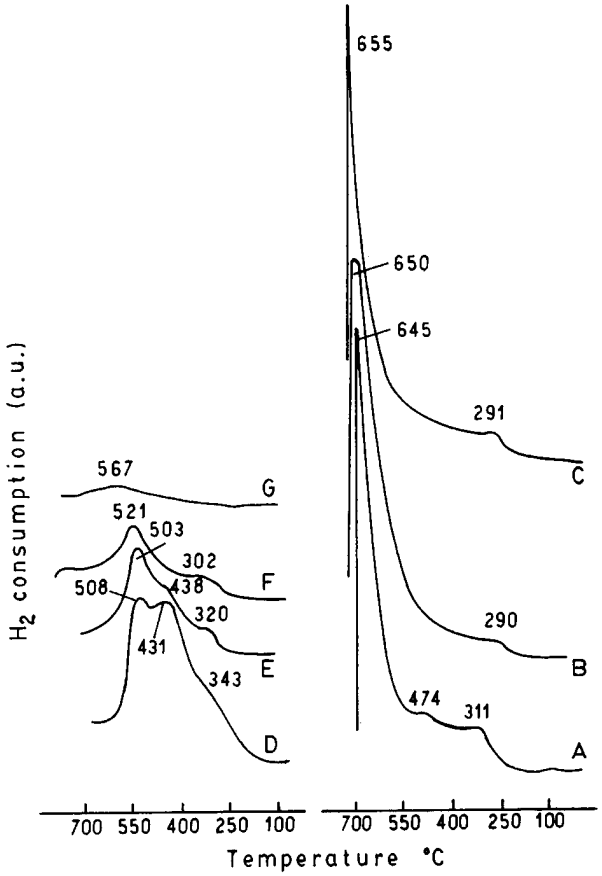

FIG. 4. Reduction profiles (TPR) measured for samples of (A) V_2O_5, (B) VT10, (C) VT20, (D) VT50, (E) VT80, (F) VT90, and (G) TiO_2. Conditions: heating rate, 5°C/min.; reducing gas mixture, 10% H_2 in N_2; gas flow rate, 55 cm^3 (NTP) min^{-1}; sample mass variable.

double bonds (Table 5); such characteristics, according to the literature (17), could be ascribed to the V(IV) oxides. Comparison of the V=O bands in the fresh and used VTiO samples indicates that the latter present lower frequencies (Table 5). This is reasonable if it is considered that, in the used catalyst, the average oxidation state of vanadium is lower than in the fresh ones, thus weakening the double bond.

Temperature-Programmed Reduction Profiles

Figure 4 shows the hydrogen consumption as a function of the temperature in the different samples and Table 4 presents the vanadium phases found in each of the reduction steps. Reduction of TiO_2 (anatase or rutile) was not observed within the temperature range. The signal appearing at 567°C in diagram G of Fig. 4 corresponds to TiO_2 dehydroxilation.

As can be seen in Fig. 4 and Table 1, the first temperature of the reduction of pure V_2O_5 occurs at 311°C. Reduction of the systems VTiO started at temperatures lower than that of V_2O_5 (VT10,VT20) or at similar values (VT80, VT90). Sample VT50, however, was the exception, since its reduction was at a higher temperature. At this reduction step we detected only surface reduction of the oxides because of a slight widening of the FTIR V=O signal (13). As it can be inferred from Table 4, the reduced titanium-containing solids have either oxides of V(IV), or a mixture of V(IV) and (V), but they were never reduced to V_2O_3 as in pure vanadium pentoxide. The titanium stabilizes vanadium oxides of intermediate oxidation state, and this could be due to the formation of solid solutions between reduced oxides and TiO_2, which are more stable than the pure crystalline structures.

Surface Characterization by XPS

Fresh catalysts. The analysis of the signals corresponding to the V_{2p} level of vanadium and the Ti_{2p} level of titanium in the XPS spectra allowed the surface oxidation states and the relative dispersion of vanadium oxide on the titania to be determined. As expected in all the 3*d*-transition metals, $V_{2p3/2}$ was the most intense vanadium photoemission. However, the precise determination of BE is difficult because the O_{1s} satellite peak interferes. As can be observed in the XPS spectrum of fresh VT10 (Fig. 5), the resolution of the $V_{2p1/2}$ level is much poorer than that of the $V_{2p3/2}$ level. Consequently, only the $V_{2p3/2}$ level was considered in the calculations. For the fresh catalysts, the locations and full width at half maximum of the vanadium $V_{2p3/2}$ and titanium $Ti_{2p3/2}$ signals, together with the V/(V + Ti) ratios, are presented in Table 1. The binding energies and FWHW of the $V_{2p3/2}$ and $Ti_{2p3/2}$ signals indicate that V(V) and Ti(IV) are present on the surface of those samples. The shift of the $Ti_{2p3/2}$ to lower B.E. coincides with those previously established by Andersson, who obtained the XPS signal of $Ti_{2p3/2}$ from mechanical mixtures of $V_2O_5 + TiO_2$ sinterized at 1100°C, at bond energy below that of pure TiO_2. At this temperature intermediate between the melting points of both oxides (V_2O_5, 690°C, and TiO_2, 1830°C) part of the TiO_2 is dissolved on the melted V_2O_5 to form a solid solution (22). The decrease in the FWHM of the VTiO catalyst signals with respect to that of pure V_2O_5 was attributed by the same author to the conductivity increase produced by formation of a solid solution.

Another relevant feature of the VTiO series appears from the comparison of bulk and surface V/(V + Ti) ratios. In vanadium-rich catalysts (VT10, VT20), the surface composition is slightly lower than that of the bulk, whereas in the vanadium-poor ones (VT50, VT80, VT90) a vanadium-enriched surface phase in present.

Used catalysts. The deconvolution of the vanadium $V_{2p3/2}$ in the used catalysts (Fig. 6) allowed us to detect the presence of V(V) and a low quantity of V(IV) on the surface of all samples, even on VT90 where the bulk V_2O_5 was not found. Table 2 shows the binding energies of the

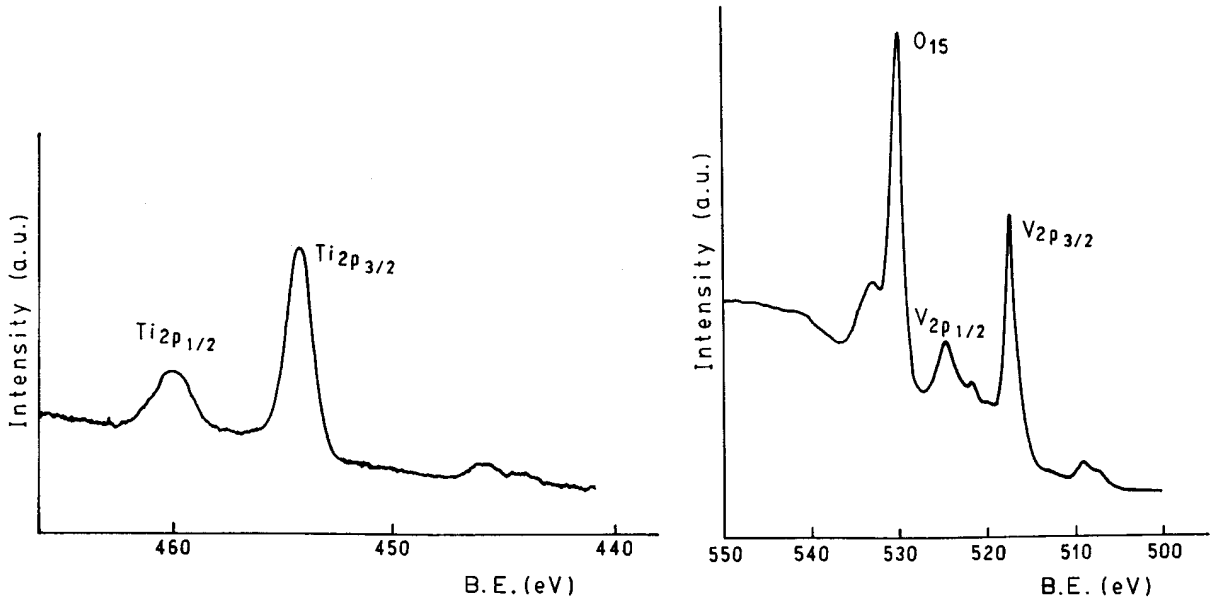

FIG. 5. Photoelectron spectra of the V_{2p} and Ti_{2p} levels of fresh VT10 catalysts.

$V_{2p3/2}$ signal of V(IV) and V(V). The titanium was not detected on the surface of the used VT10 and VT20 catalysts; its oxidation state did not change in the other samples. Comparison between the vanadium dispersion in the fresh samples and that in the used samples showed that the latter were surface-enriched in vanadium, except in sample VT80, which remained unchanged.

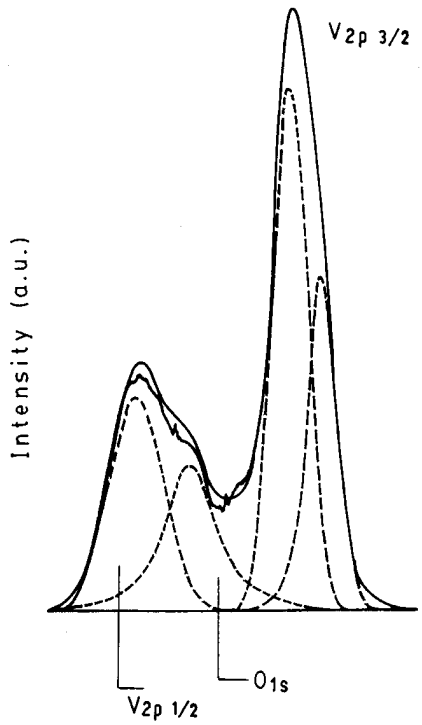

FIG. 6. Photoelectron spectra of the V_{2p} levels of used V_2O_5 catalyst. Dotted lines correspond to the peak identified by the deconvolution process.

Morphological Characterization by SEM

Fresh catalysts. Photographs 1a, 2a, and 3a show the characteristic morphology of particles of the fresh catalysts. Samples VT10 and VT20 exhibit plate- and needle-shaped particles, corresponding to the plane (001) of V_2O_5 (23). In catalysts VT50, VT80, and VT90, small needles on large TiO_2 granules are observed. Titanium modifies the morphology of the V_2O_5 phase, the extent of that effect depending on the TiO_2 concentration. As the TiO_2 concentration increases, the contribution of plane (001) becomes progressively smaller, as observed in the XRD spectra (Fig. 1). The bottom right angle of the photographs presents a detailed view of the isolated particles of the catalysts. It is evident that, as the ratio V/(V + Ti) increases, the catalyst morphology changes from a rectangular shape—characteristic of the vanadium pentoxide—to a granular shape, which is typical of the titanium dioxide.

Used catalysts. After being used in the reaction, the solids do not modify their morphology (photographs 1b, 2b, 3b).

Active Surface Area: Oxygen Chemisorption

Figures 7 to 12 present the oxygen consumption, expressed in mole per unit area of the solids, and the linear regression of such data on temperature and number of oxygen pulses. The amount of chemisorbed oxygen is sensitive to the pulse volume; this can be inferred from the rapid saturation observed in the VT50 catalysts (Fig. 10) when a 1.00 ml

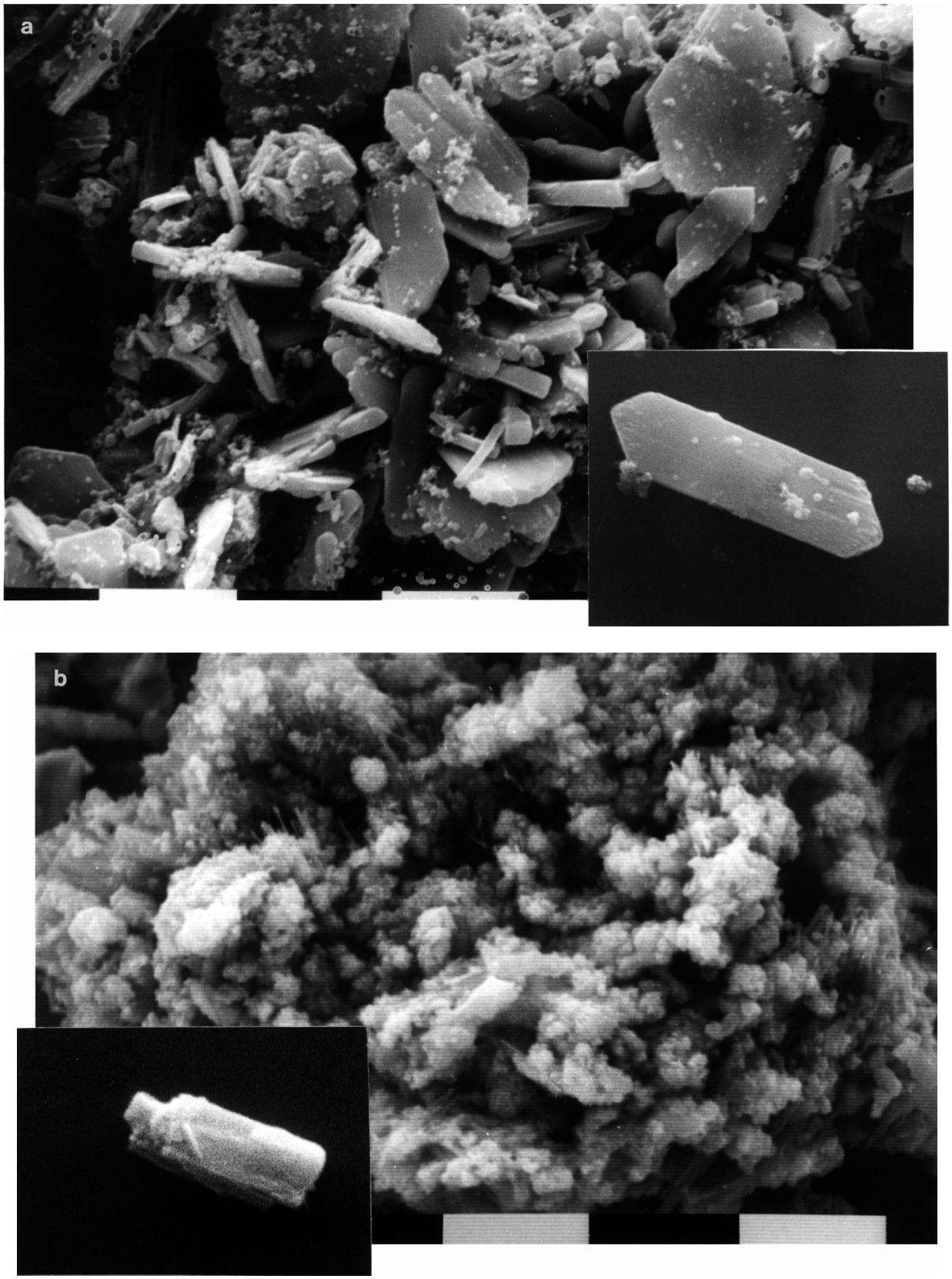

PHOTOGRAPH 1. Morphology of (a) fresh VT10 catalyst (× 2000); (b) used VT10 catalyst (× 2000). Bottom corners: (a) isolated fresh ($\times 1 \times 10^{-4}$) and (b) used ($\times 1 \times 10^{-4}$) catalyst particles.

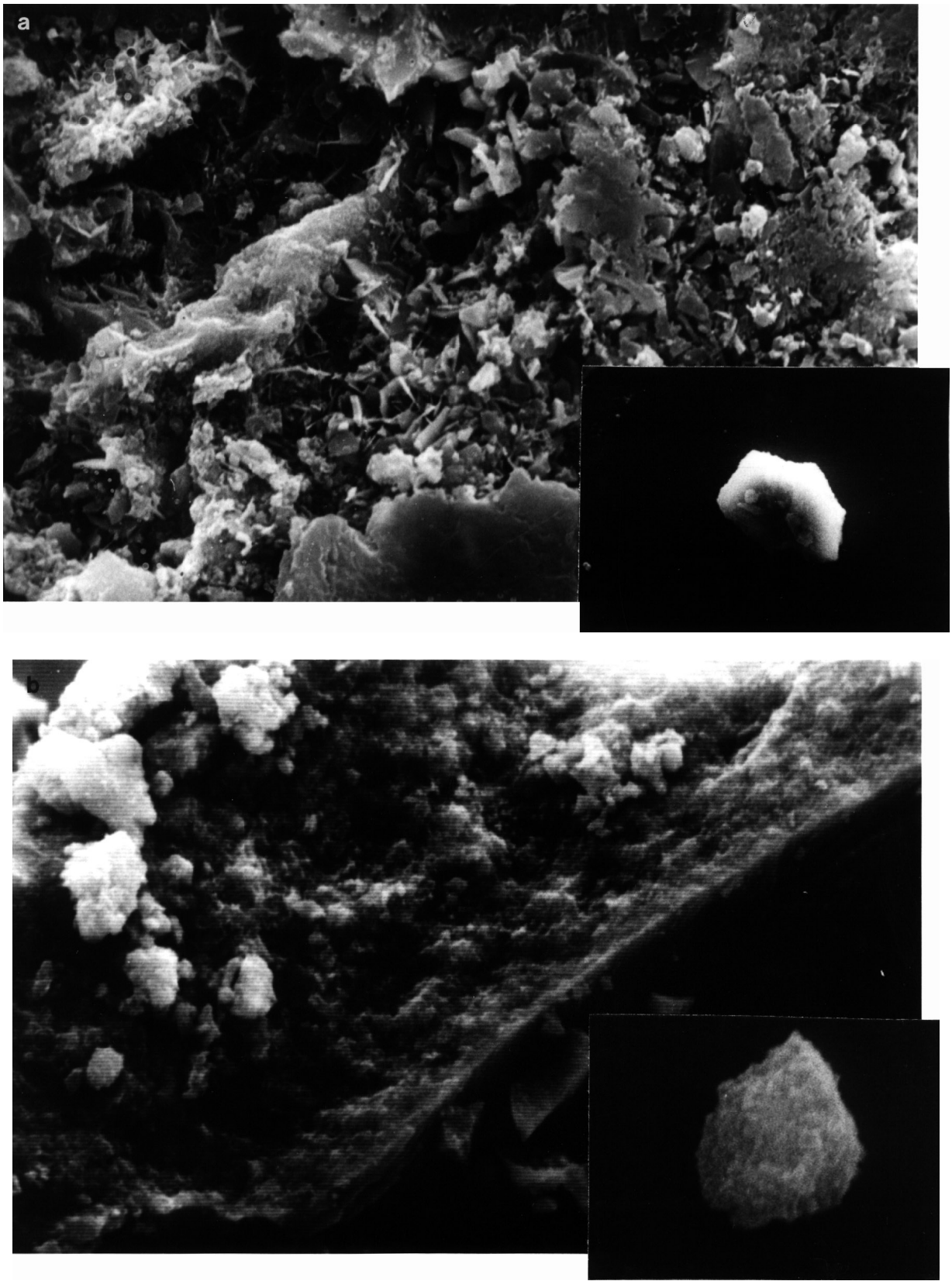

PHOTOGRAPH 2. Morphology of (a) fresh VT50 catalyst (× 2000); (2.b.) used VT50 catalyst (× 2000). Bottom corners (a) isolated fresh (× 1490) and (b) used catalyst (× 10,400) particles.

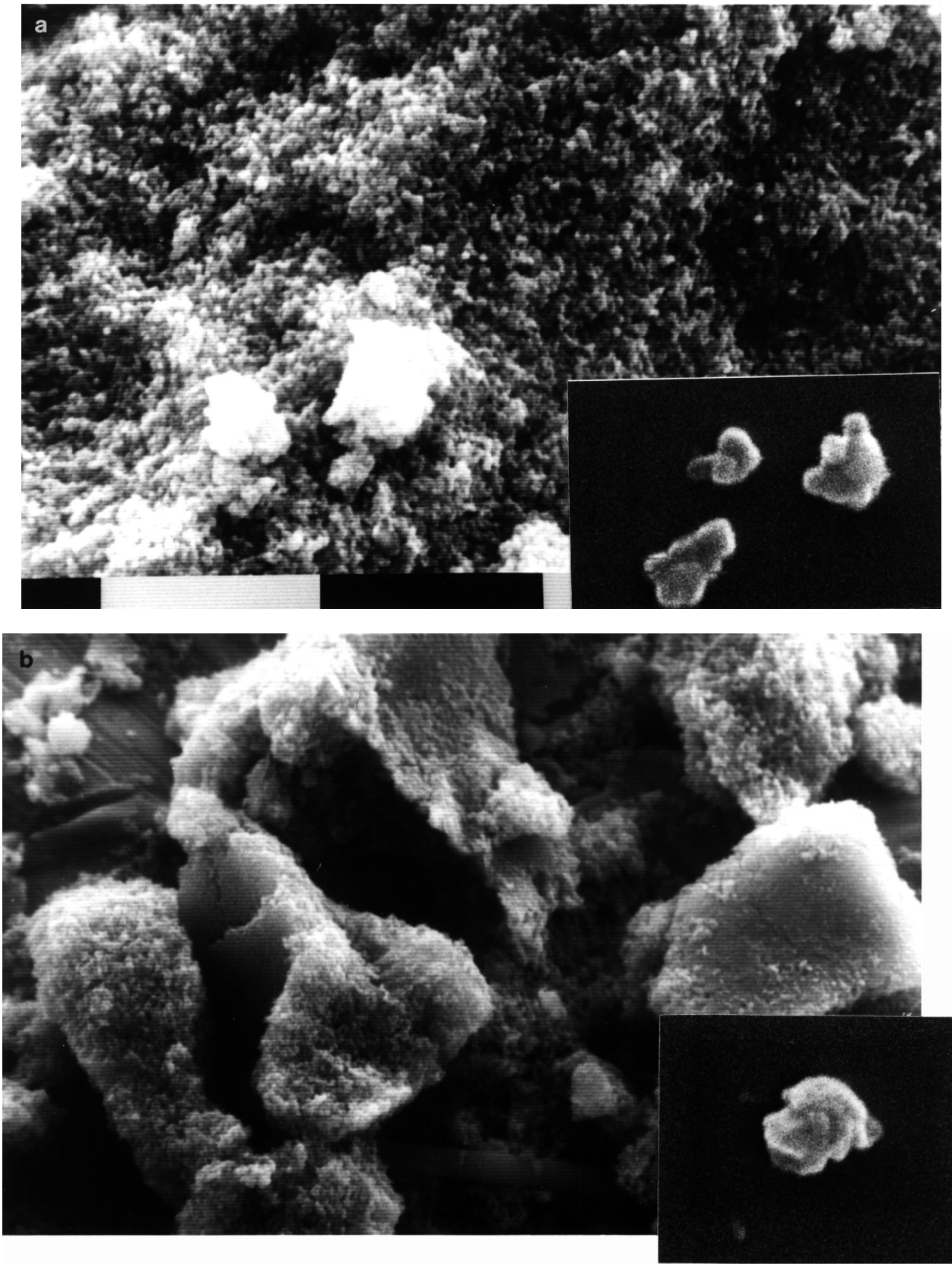

PHOTOGRAPH 3. Morphology of (a) fresh VT90 catalyst (x 2000); (b) used VT90 catalyst (× 2000). Bottom corners: (a) isolated fresh ($\times 2 \times 10^{-4}$) and (b) used ($\times 2 \times 10^{-4}$) catalyst particles.

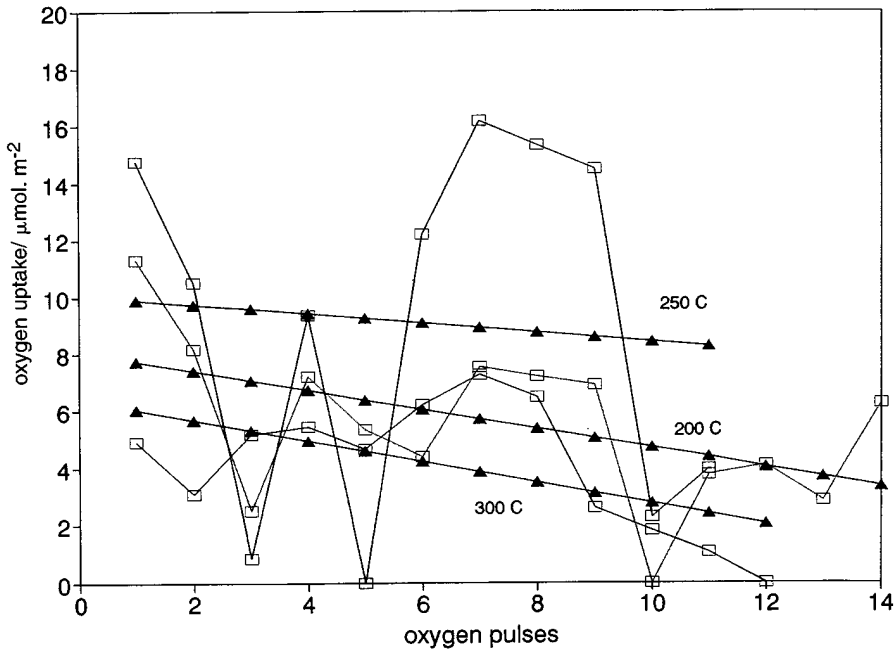

FIG. 7. Oxygen uptake curves on V_2O_5 at different temperatures. Symbols: □ oxygen consumption per pulse, △ linear regression of such data.

pulse is used. Therefore, we decided to use 0.50 ml pulses in all cases. As a consequence of the successive oxygen pulses, the behavior of the samples is such that there was discontinuous variation of the process, with some periods of stronger adsorption and some others of weaker adsorption, which are ascribed to a high relaxation time in the structures. With the exception of samples V_2O_5 and VT10, the TCD did not show evidence of oxygen desorption. The linear regression of the data demonstrates the slowness of the process; moreover, the amount of adsorbed oxygen decreases to an almost null value after 20 pulses at least. On the other hand, the temperature increase activates the chemisorption phenomenon and increases the total amount of consumed oxygen as well. This fact were also observed by previous authors in the vanadium–titanium system (18). With the exception of V_2O_5 and VT10, the oxygen consumption was low at

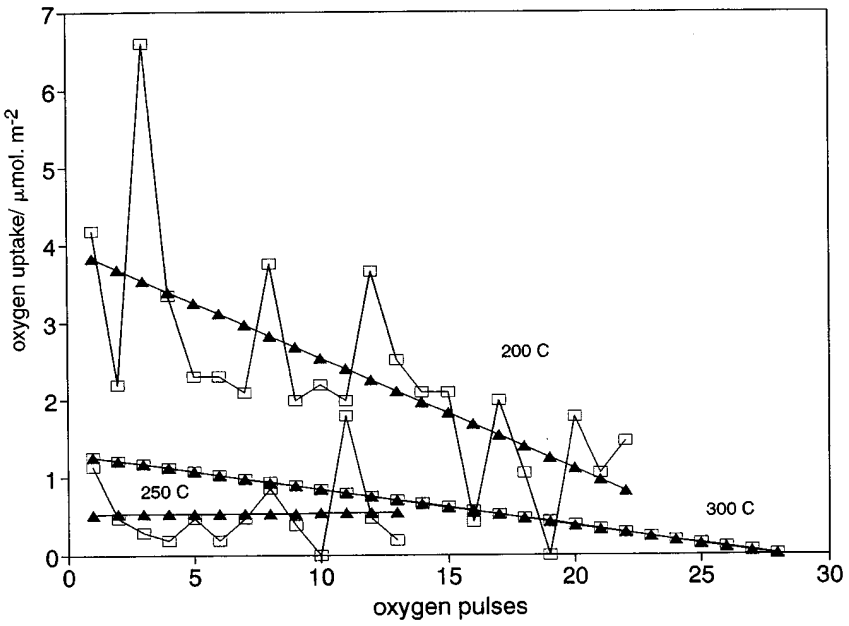

FIG. 8. Oxygen uptake curves on VT10 at different temperatures. For symbols see Fig. 7.

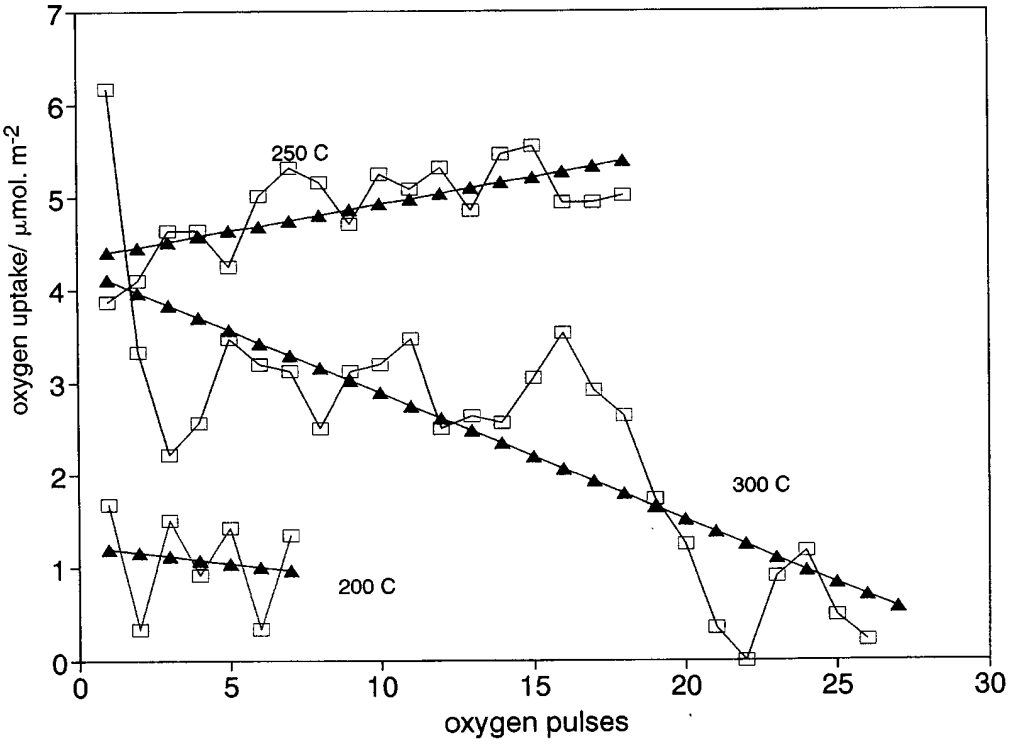

FIG. 9. Oxygen uptake curves on VT20 at different temperatures. For symbols see Fig. 7.

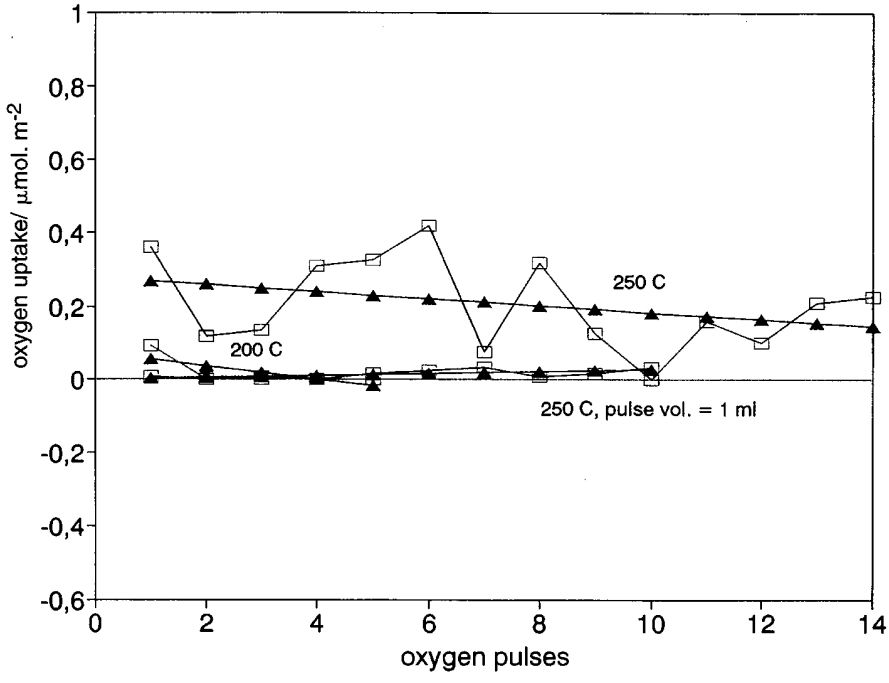

FIG. 10. Oxygen uptake curves on VT50 at different temperatures. For symbols see Fig. 7.

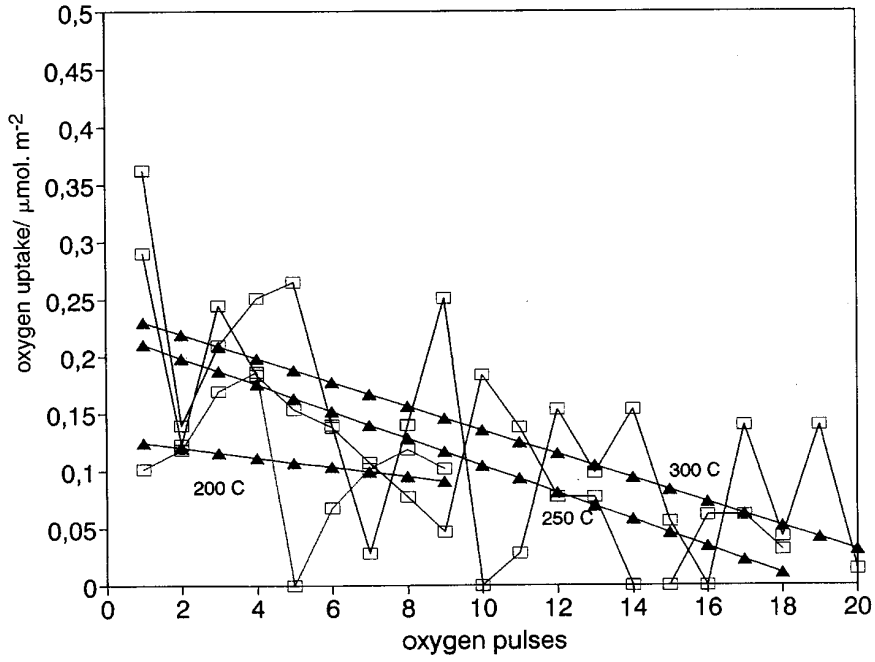

FIG. 11. Oxygen uptake curves on VT80 at different temperatures. For symbols see Fig. 7.

200°C, and increased from 250°C onward. This result is not surprising since, at the latter temperature, a maximum of surface-chemisorbed oxygen was observed in experiments carried out by the volumetric method. We will comment on such tests in subsequent sections (20, 21).

In the samples V_2O_5 and VT10, the maximum O_2 adsorption takes place at 200°C, whereas, at higher temperatures, the oxygen is desorbed immediately after the pulse (Figs. 7, 8).

Oxidation of Methanol over Pure V_2O_5 and V_2O_5–TiO_2 Catalysts

Products of the selective oxidation of methanol on V_2O_5 were formaldehyde, dimethyl ether, CO, and CO_2. Figure 13

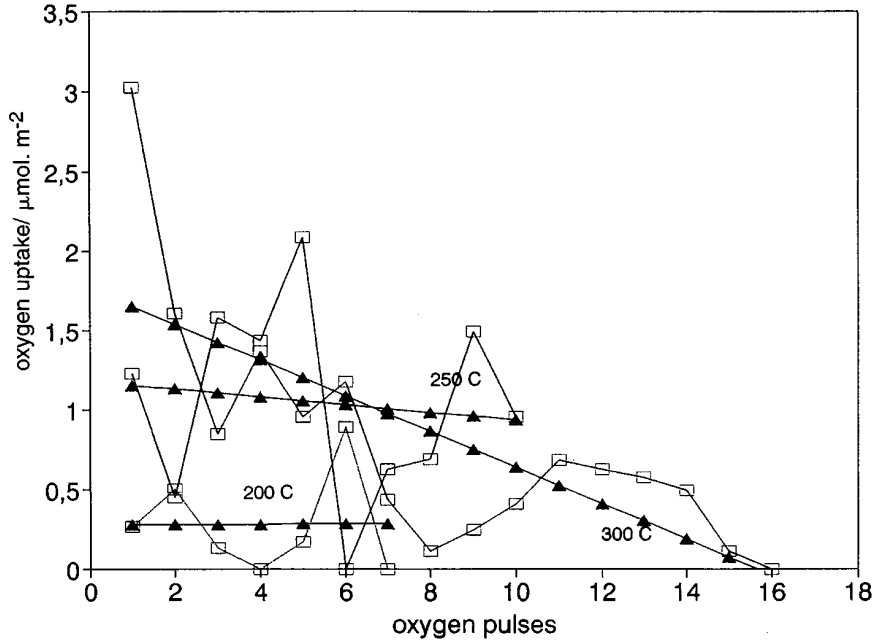

FIG. 12. Oxygen uptake curves on VT90 at different temperatures. For symbols see Fig. 7.

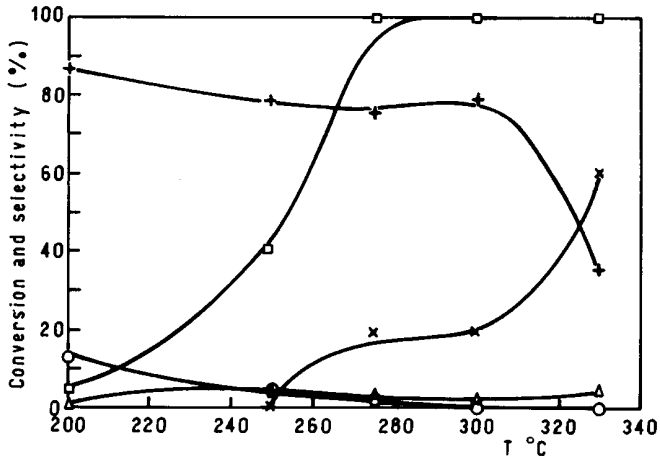

FIG. 13. Selective oxidation of methanol on V_2O_5 catalyst at constant feed contact time (0.8 sec) and methanol concentration in air (10 moles CH_3OH/air %). Symbols: □ methanol conversion %, + CH_2O selectivity %, ■ $(CH_3)_2O$ selectivity %, △ CO_2 selectivity %, and × CO selectivity %.

shows that within the range from 200 to 275°C, the conversion increased from about 3% to 100%, while the selectivity to HCHO remained at a constant value of approximately 80% up to temperatures of 300°C. The production of CO was opposite to that of formaldehyde; that is, the selectivity to the monoxide was null at 250°C, increased to 20% at 300°C, and to higher values for increasing temperatures, while at the same time, the selectivity to formaldehyde decreased.

On the other hand, at the same time, there was $(CH_3)_2O$ production with a maximum selectivity of 14%, whereas carbon dioxide production was detected in the whole temperature range under study, with a constant selectivity never above 7%.

TiO_2 anatase exhibited high activity in partial oxidation of methanol only at about 300°C. At this temperature, 100% activity, was reached to produce 80% CO and 18% CO_2.

Apart from products obtained with pure vanadium pentoxide, the VTiO catalysts produced methylal and methyl formate. VT10 and VT20 (Figs. 14 and 15, respectively) start converting methanol at temperatures higher than 200°C while, at about 280°C, almost all the methanol is converted to CO. Samples VT50, VT80, and VT90 (Figs. 16, 17, and 18, respectively) are active at a slightly lower temperature (180°C), and they also convert all the methanol to CO at a temperature of 250°C, a value lower than that previously mentioned. Within these temperature ranges the major products were formaldehyde, methyl formate, and CO.

At low temperatures, methylal was also found, together with the major products of samples VT20, VT50, and VT80. Minor products were dimethyl ether and CO_2, which remained at low and constant selectivities, almost unaltered by either the temperature or the production of the other

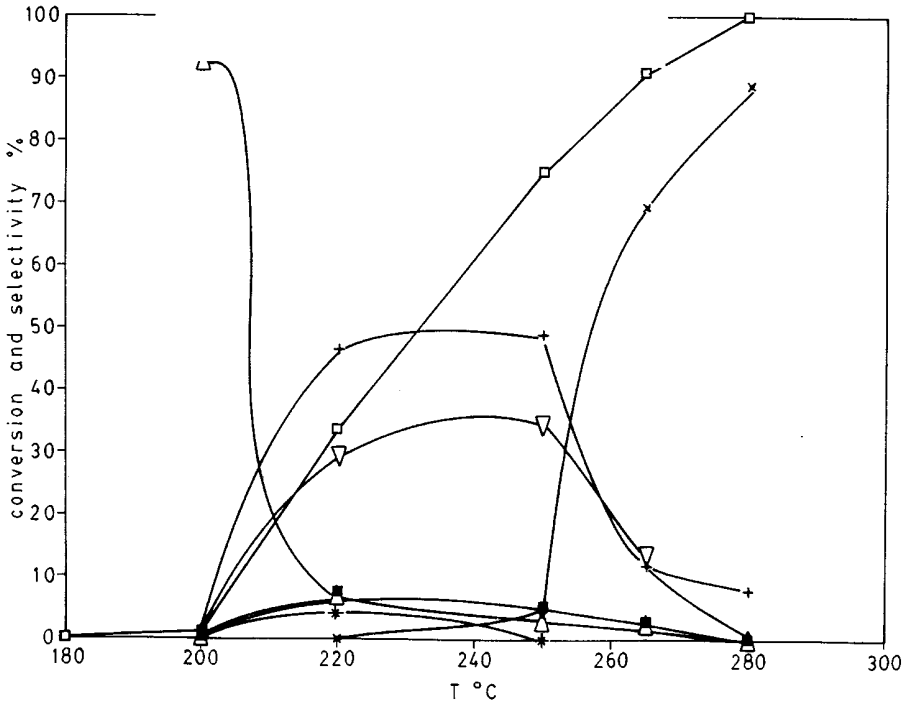

FIG. 14. Selective oxidation of methanol on VT10 catalyst at constant feed contact time (0.8 sec) and methanol concentration in air (10 moles CH_3OH/air %). Symbols: □ methanol conversion %, + CH_2O selectivity %, ■ $(CH_3)_2O$ selectivity %, ▽ methyl formate selectivity %, ● methylal selectivity %, ∗ formic acid selectivity %, △ CO_2 selectivity %, and × CO selectivity %.

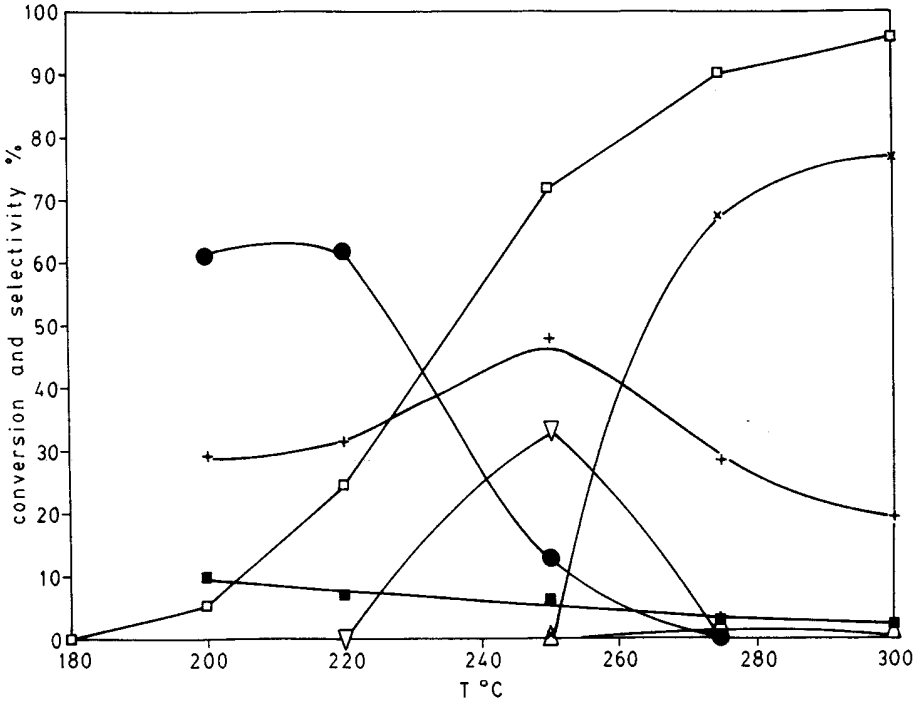

FIG. 15. Selective oxidation of methanol on VT20 catalyst at constant feed contact time (0.8 sec) and methanol concentration in air (10 moles CH_3OH/air %). For symbols see Fig. 4.

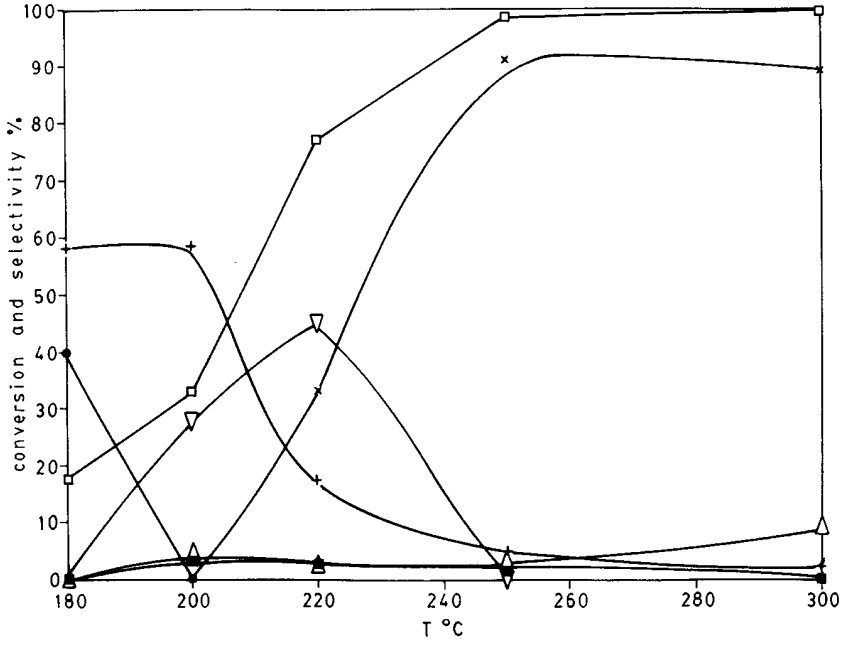

FIG. 16. Selective oxidation of methanol on VT50 catalyst at constant feed contact time (0.8 sec) and methanol concentration in air (10 moles CH_3OH/air %). For symbols see Fig. 4.

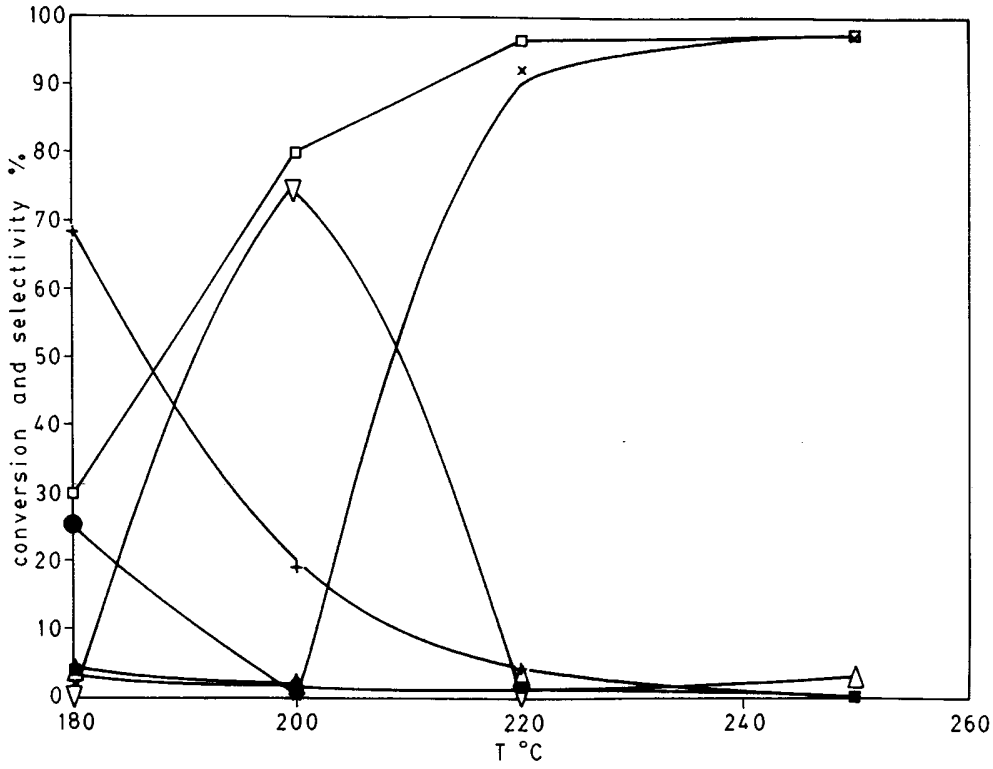

FIG. 17. Selective oxidation of methanol on VT80 catalyst at constant feed contact time (0.8 sec) and methanol concentration in air (10 moles CH_3OH/air %). For symbols see Fig. 4.

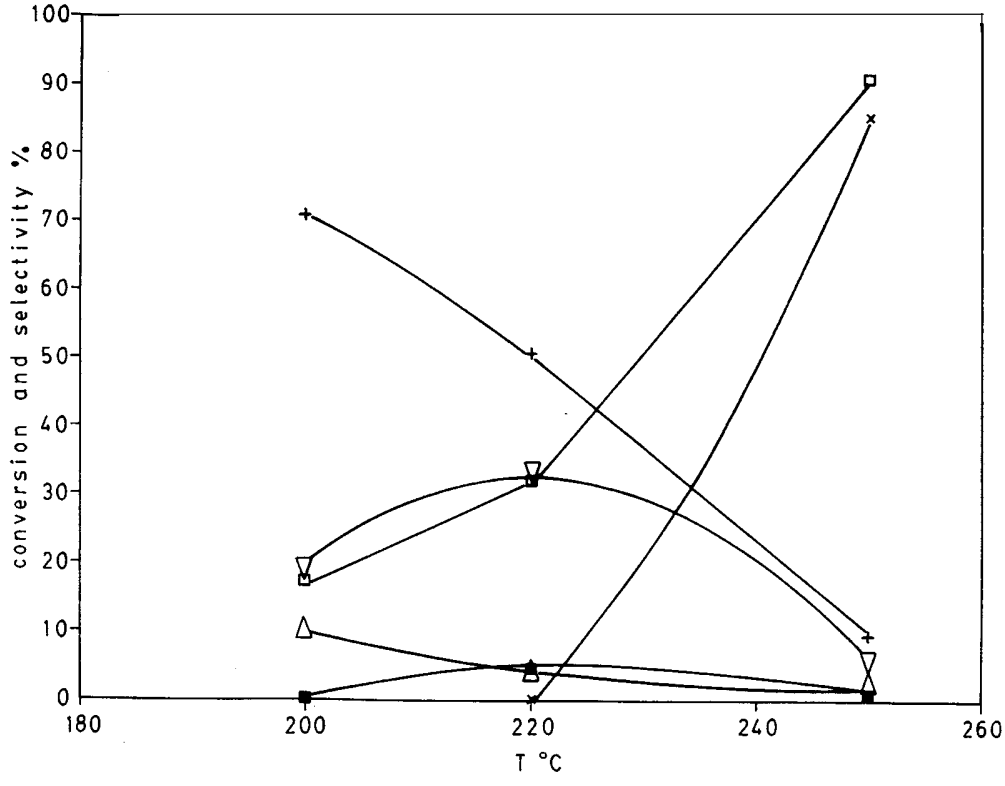

FIG. 18. Selective oxidation of methanol on VT90 catalyst at constant feed contact time (0.8 sec) and methanol concentration in air (10 moles CH_3OH/air %). For symbols see Fig. 4.

products. Only the sample VT10 produced a small amount of formic acid at low temperatures.

With regard to the influence of the contact time of the feed mixture on the activity and selectivity of this catalytic system, the studies showed clearly that increased contact time improves methanol conversion and the selectivities to methyl formate, methylal and CO at the expense of a decrease in the selectivity to formaldehyde (24). By virtue of these results we can deduce that formaldehyde is the first product of methanol partial oxidation and an intermediate species in the generation of methyl formate, methylal, and CO, and on the other hand, that dimethyl ether and CO_2 are produced in reaction steps that do not depend on the production of the major products. Therefore, under the differential reaction conditions, the complex reaction scheme of methanol oxidation over VTiO catalysts can be simplified to the selective oxidation of the alcohol to HCHO. Owing to the reactivity of this catalytic system at temperatures above 200°C, the activity measurements under differential conditions (conversion below 10%) were conducted at 150°C and at different contact times of the feeding mixture to keep the conversion low.

DISCUSSION

State of Vanadia

As a consequence of the different analysis conducted on the fresh catalysts, the results indicate that the distribution of the titanium and vanadium phases depends strongly on the V/(V + Ti) ratio. The catalysts with high vanadium concentrations (VT10, VT20) show rectangular particles, which are similar to those of pure vanadium pentoxide. However, the surface concentration of vanadium is lower than that in the bulk, so it is reasonable to deduce that, during the preparation, the V_2O_5 precipitated first and the titanium dioxide second, thus partially covering the vanadium phase. Therefore, the particles of these catalysts would have big crystals of V_2O_5 in the center in contact with small crystals of a solid solution of vanadium in anatase and rutile, which partially cover the surface of the particles. In catalysts VT50, VT80, and VT90, the situation is opposite: the titanium dioxide precipitates first as anatase and rutile in solid solution with vanadium, and then the V_2O_5. For this reason, a spherical morphology—characteristic of titanium—and a higher concentration of vanadium are observed. As the titanium is also observed in the surface of these catalysts, we infer that the V_2O_5 particles do not totally cover the titanium surface; moreover, the titanium would act as a support for small isolated crystals of vanadium pentoxide.

Previous studies of the different phases that make up the coprecipitated VTiO and supported V/TiO_2 catalysts have indicated the possibility of formation of an amorphous phase of V(V) species in strong interaction with the titanium surface by Ti–O–V(25–29). In fact, recent studies of the fresh VTiO catalysts, from which the crystalline V_2O_5 was removed by washing in a basic medium, showed the presence of VO_x species covering the surface of the titanium phase (30).

The trend of the first reduction temperature in VTiO is related to the vanadium surface dispersion. Catalysts VT10 and VT20, whose surface vanadium concentration [V/(V + Ti) is 0.82, 0.84, respectively] is higher than those in the rest of the series, are composed of vanadium in solid solution with the titanium, though with particularly large vanadium pentoxide crystals, very similar in morphology to those of vanadium pentoxide. This extended surface is less influenced by the titanium, and is more easily reached by the hydrogen, unlike in the rest of the catalyst series, where a lower surface vanadium concentration suggests that this phase is in small and isolated crystals, in closer contact with the titanium dioxide crystals. Such a greater vanadium–titanium interaction is also observed in the shift of the V=O double bond signal to higher infrared frequencies produced by an increase of titanium concentration. Such bonds are directly involved in the temperature-programmed reduction process, so it is reasonable to see that catalysts exhibiting V=O species with stronger—and therefore less labile—bonds are less reducible.

During reaction, three fundamental processes occur on the surface of the catalysts: (1) vanadium diffusion to the bulk with consequent variation of the network parameters of anatase (VT90) and rutile (VT20, VT90); (2) surface vanadium migration, leading to an increase of the surface ratio V/(V + Ti); and (3) reduction of the V(V) to V(IV), which also takes place in the bulk of the crystals. With regard to the last point, we can say that the crystalline V_2O_5 was reduced to crystalline oxides of V(IV) and, possibly, to intermediate oxidation states, as demonstrated by the XRD diagrams of the used catalysts. Bearing in mind that the fresh catalysts had VO_x species covering the titanium surface, a possible fact is an increase of this phase by surface migration of vanadium during the chemical reaction, because of which an increase of the V/(V + Ti) surface ratio was observed in the used catalysts.

The photographs of the used catalysts and their isolated particles indicate that the used catalysts VT10 and VT20 maintained the morphology they originally had.

Catalytic Behavior

As established in the previous section, the used catalysts have crystalline V_2O_5, V(IV) oxides and an amorphous phase of VO_x species composed of V(V). The activity and selectivity results that were previously commented on suggest that only the vanadium phases are active in the selective oxidation of methanol on VTiO catalysts and that the presence of titanium leads to the production of more complex condensation substances (methylal and methyl formate). This is observed in Fig. 19, which compares the selectivities

of V_2O_5 and VTiO catalysts to the partial oxidation products at 50% conversion. It is evident that the presence or absence of titanium in the used catalysts (Table 2) do not modify the production of one or another product, since no correlation is observed between the surface dispersions of the different catalysts and their selectivities.

In our laboratory, we did some experiments to asses the catalytic activity of the VO_x species. To this end, we utilized the fresh catalysts VT50 and VT90, which were washed with an ammonia solution to remove the crystalline vanadium pentoxide. The resultant solid is composed of a solid solution with TiO_2 covered by VO_x species. In the sample VT50, the methanol was totally oxidized to CO_2. However, the catalyst VT90 led, at 250°C, to 7% CO_2, 29% HCHO, and 60% methyl formate with 16% conversion, whereas at 300°C, it showed a conversion of 78%, leading to 9% CO_2, 17% HCHO, and 75% methyl formate. Such differences of behavior between the washed and used solids, and, in addition, among washed, and among used, suggest the following conclusions: (1) the amorphous phase of VO_x species is active in the methanol oxidation, (2) that more than one type of VO_x species may be present, and (3) that the surface may not be completely covered by such species (2, 31).

Activity Dependence on Chemisorption Sites and Strength of V=O Sites

The concentration of active sites in systems such as transition metal oxides, the surfaces of which are somewhat unstable (nonstoichiometric), is difficult to quantify. Nevertheless, conclusions drawn from studies of oxygen chemisorption on V_2O_5 and on the coprecipitated V_2O_5–TiO_2 systems, conducted in our laboratory (20, 21), made it possible to relate the sites involved in the chemisorption to those involved in the partial oxidation of methanol. These relationships are summarized below:

1. Only vanadium-containing phases participate in oxygen chemisorption. Moreover, it is well known that the O_2 reoxidizes the V=O species while undergoing dissociation and adsorption of one oxygen atom per reduced vanadium site (18, 19, 32–36).
2. Two maxima, one at 250°C and another at 400°C, were observed in the adsorption isobars of oxygen. The first was assumed to belong to the oxygen chemisorption process on the surface-reduced sites; the second is due to the effect of oxygen diffusion from the surface to the bulk or to diffusion of vacancies from the bulk to the surface.
3. At 250°C, the amount of adsorbed oxygen per gram of V_2O_5 depends on the sample composition, decreasing in the following order: VT80, VT50, VT10, VT20, and V_2O_5.
4. The kinetics of oxygen chemisorption indicated two different and consecutive adsorption processes taking place between 200 and 350°C. These differences result from the existence of two—either energetically or/and structurally different–types of sites.

The partial oxidation of methanol is used to prove the reactivity of the surface vanadium redox sites (2). The methanol chemisorbs on vanadium oxide catalysts as a surface methoxy (CH_3O) and, depending on the nature of the sites present on the surfaces of the catalyst, can react via various pathways to form formaldehyde, methyl formate, methylal, dimethyl ether, or carbon oxides. Several authors have shown that the partial oxidation of hydrocarbons over V_2O_5 phase takes place on two different sites (37, 38):

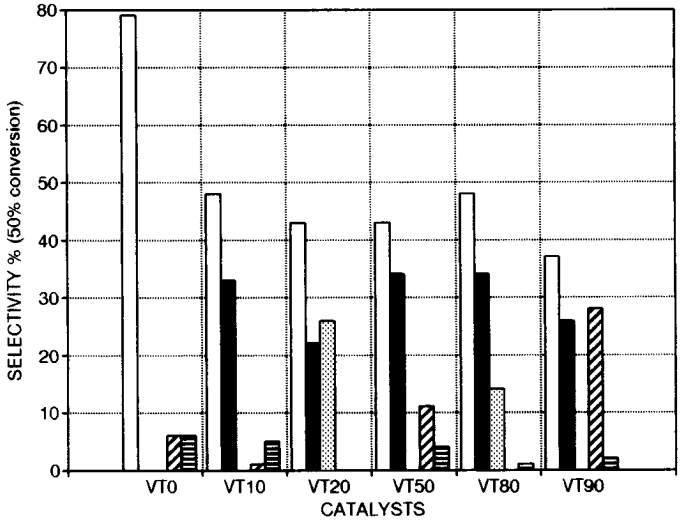

FIG. 19. Selectivities of methanol partial and total oxidation products, at 50% conversion. Symbols: □ CH_2O selectivity %; ▤ CO_2 selectivity %; ▨ methylal selectivity %; ▨ CO selectivity %; ■ methyl formate selectivity %.

double bounded vanadyl sites, active centers for oxidation

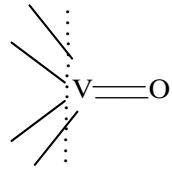

and exposed vanadium atoms, with Lewis acid character

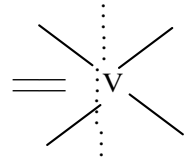

According to these results, it could be thought that the sites actually involved in the O_2 chemisorption process are the same as those participating in the adsorption and further partial and/or total oxidation of methanol. The active surface was calculated, depending on the chemisorption stoichiometry, as twice the total moles of adsorbed oxygen per unit area of the catalyst, at the minimum temperature at which the oxygen adsorption was evidenced. These temperatures were above that of the catalytic tests conducted un-

der differential conditions because chemisorption is an activated process. The concentration of active sites, the reaction rates, and the turnover numbers (TON) are presented in Table 6, the reaction rate being defined as the amount of methanol converted in the differential experiments, per time unit and surface area of each catalyst. The turnover numbers were defined as reaction rate per adsorption sites concentration in the catalysts. When turnover numbers are used, we are expressing the activities per active site, thus eliminating the variation introduced by changes in the number of active sites. Therefore we use TON values to compare the modifications of the catalytic properties of each site.

As it can be seen, the activity (reaction rate) of the catalysts increases with the surface concentration of sites and therefore shows behavior opposite to the vanadium surface dispersion. These observations are in agreement with the fact that titanium is not an active site on the partial oxidation of methanol, as previously established in the discussion about activity and selectivity under integral reaction conditions. However, the VTiO catalysts generate selective oxidation products (methyl formate, methylal) which are more complex than those of pure vanadium pentoxide. At this point, the titanium plays an important role which is reflected in a twofold decrease of the turnover number of the VTiO with respect to that of vanadium pentoxide. If the TON values of VTiO are compared, similarity is observed between the values for the catalysts VT50, VT80, and VT90. As previously remarked, these solids would have a morphology similar to that of supported catalysts, so a stronger vanadium–TiO_2 interaction is possible. In fact, in the last catalysts, the reduction temperature is higher than that of pure vanadium pentoxide, which would indicate that the surface sites V=O are less reducible because of its stronger double bonds. Therefore, they have a lower capacity to react with hydrogen to form hydroxyl ions:

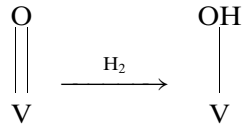

TABLE 6

Reaction Rates, Active Sites (Oxygen Chemisorption Temperature at Which They Were Calculated) and Turnover Frequency, of Used V_2O_5 and VTiO Catalysts

Sample	Reaction rate (mol m^{-2} sec^{-1})	Sites (Chem. Temp.°C) (mol m^{-2})	TON (sec^{-1})
V_2O_5	1.15×10^{-4}	1.21×10^{-4} (200)	0.94
VT10	6.11×10^{-5}	8.75×10^{-5} (200)	0.70
VT20	5.81×10^{-5}	1.19×10^{-4} (300)	0.49
VT50	2.47×10^{-6}	4.39×10^{-6} (250)	0.56
VT80	2.14×10^{-6}	3.66×10^{-6} (250)	0.58
VT90	7.19×10^{-6}	1.35×10^{-5} (250)	0.53

The trend of reduction temperatures is also observed in the increase of the IR frequencies of the double bond V=O in both fresh and used catalysts.

On the other hand, to produce HCHO, the methanol must be adsorbed on an acid site through its oxygen atom and then it must be dehydrogenated by adsorption and reaction with the adjacent V=O sites. Bearing this mechanism in mind, it would be reasonable to think that the solids with less reactive redox sites (of lower dehydrogenation capacity) would stabilize the adsorbed HCHO intermediate of the mechanism proposed by Sambeth *et al*. (8, 9):

$$\begin{array}{lcl} CH_3OH_g \xrightarrow{I} CH_3OH_{ad} & \xrightarrow[O_2]{II} & HCHO_{ad} \xrightarrow{III} HCHO_g \\ & & \text{IV} \downarrow CH_3OH_g \\ HCOOCH_3 & \xleftarrow[O_2]{} & CH_3OCH_2OH_{ad} \xrightarrow[CH_3OH]{} CH_3OCH_2OCH_3 \end{array}$$

The greater stability of the intermediate [$HCHO_{ad}$] would facilitate further condensation with other methanol molecule to form hemimethylal. The stability of the adsorbed intermediate also depends on the acid sites of Lewis, because of which the final verification of the mechanism is linked to the measurement of the quantity and quality of such sites. The fact that the titanium modifies these sites would explain why the V_2O_5 does not produce methylal or methyl formate despite having a surface reduction temperature similar to that of catalyst VT90.

The greater stability of the intermediate was also verified by Sambeth *et al*. (8, 9). These authors observed that the hemimethylal was generated within the first minutes of methanol–VTiO contact, unlike in V_2O_5, where hemimethylal was detected only after several hours of contact.

CONCLUSION

The reaction of methanol in a stoichiometric excess of air on coprecipitated vanadium–titanium oxides produces HCHO as a first step and then, from it, methyl formate, methylal, and carbon monoxide. Bearing in mind the inactivity of TiO_2, it can be assumed that only vanadium-containing phases are active in the reaction. After the reaction, the catalyst surfaces, were enriched in vanadium, which was found mainly as V(V). The reaction rate of the partial oxidation of methanol is directly proportional to the concentration of such sites and it vanishes when titanium is present only on the surface. On the other hand, in the selective oxidation of methanol to HCHO, under differential conditions (low temperatures and long contact times), the catalyst activity decreases with increasing V=O energy. These results indicate that the reaction rate would be controlled by a strong methanol adsorption on the catalyst surface which, in turn, inhibits the next step of the reactant oxidation.

ACKNOWLEDGMENTS

The authors are grateful to Mrs. Graciela Valle for performing the infrared analysis, to Ing. Laura Cornaglia for the XPS analysis, and to Professor Carlos Gigola for his valuable comments.

REFERENCES

1. Centi, G., Perathoner, S., and Trifiró, F., *Res. Chem. Intermed.* **15**, 49 (1991).
2. Deo, W., and Wachs, I., *J. Catal.* **146**, 323 (1994).
3. Slinkard, W. E., and DeGroot, P. B., *J. Catal.* **68**, 423 (1981).
4. Fierro, J. L. G., Arrua, L. A., Lopez Nieto, J. M., and Kremenic, G., *Appl. Catal.* **37**, 323 (1988).
5. Cavani, F., Centi, G., Parrinello, F., and Trifiró, F., *Stud. Surf. Sci. Catal.* **31**, 227 (1987).
6. Cavani, F., Foresti, E., Trifiró, F., and Busca, G., *J. Catal.* **106**, 251 (1987).
7. Forzatti, P., Tronconi, E., Busca, G., and Tittarelli, P., *Catal. Today* **1**, 209 (1987).
8. Sambeth, J., Gambaro, L., and Thomas, H., *in* "Proceedings of the XIV Simposio lberoamericano de Catálisis, Chile, 1994," Vol. 2, p. 951.
9. Sambeth, J., Gambaro, L., and Thomas, H., *Adsorpt. Sci. Technol.* **12**, 171 (1995).
10. "ASTM Powder Diffraction File," Joint Committee on Powder Diffraction Standards, Philadelphia, 1993.
11. Seiyama, T., Nita, K., Maehara, K., Yamazoe, N., Takita, Y., *J. Catal.* **49**, 164 (1977).
12. Klug, H. P., and Alexander, L. E., "X-Ray Diffraction Procedures for Polycrystalline and Amorphous Materials," Wiley, New York, 1976.
13. Briand, L., Gambaro, L., and Thomas, H., *J. Therm. Anal.* **44**, 803 (1995).
14. Frederickson, L., and Hausen, M., *Anal. Chem.* **35**, 818 (1963).
15. Fabri, G., and Baraldi, P., *Anal. Chem.* **44**, 1325 (1972).
16. Theobald, F., *Rev. Roum. Chem.* **23**, 887 (1978).
17. Barraclough, C. G., Lewis, J., and Nyholm, R. S., *J. Chem. Soc.* 3552 (1951).
18. Oyama, S. T., Went, G. T., Lewis, K. B., Bell, A. T., Somorjai, G. A., *J. Phys. Chem.* **93**, 6786 (1989).
19. Oyama, S. T., *J. Catal.* **128**, 210 (1991).
20. Rey, L., Martino, R., Gambaro, L., and Thomas, H., *Adsorpt. Sci. Technol.* **5**, 280 (1988).
21. Quaranta, N., Gambaro, L., and Thomas, H., *J. Catal.* **107**, 503 (1987).
22. Andersson, L., *J. Chem. Soc. Faraday Trans. 1* **75**, 1356 (1979).
23. Baiker, A., and Monti, D., *J. Catal.* **91**, 361 (1985).
24. Briand, L., Gambaro, L., and Thomas, H., *React. Kinet. Catal. Lett.* **52**, 169 (1994).
25. Cavani, F., Genti, G., Parrinello, F., and Trifiró, F., *Stud. Surf. Sci. Catal.* **31**, 227 (1987).
26. Cavani, F., Foresti, F., Parrinello, F., and Trifiró, F., *Appl. Catal.* **49**, 311 (1988).
27. Wachs, I., Saleh, R., Chan, S., and Chersich, C., *Appl. Catal.* **13**, 339 (1985).
28. Saleh, R., Wachs, I., Chan, S., Chersich, C., *J. Catal.* **98**, 102 (1986).
29. Cristiani, C., and Forzatti, P., *J. Catal.* **116**, 586 (1989).
30. Briand, L., Cornaglia, L., Güida, J., and Thomas, H., *J.Mater. Chem.,* 1443 (1995).
31. Went, G. T., Leu, L., and Bell, A., *J. Catal.* **134**, 479 (1992).
32. Nag, N. K., Chary, K. V. R., Reddy, B. M., Rao, B. R., Subrahmanyam, V. S., *Appl. Catal.* **9**, 225 (1984).
33. Nag, N. K., Chary, K. V. R., Reddy, B. M., Rao, B. R., Subrahmanyam, V. S., *Appl. Catal.* **31**, 73 (1987).
34. Rey, L., Martino, R., Gambaro, L., and Thomas, H., *React. Kinet. Catal. Lett.* **28**, 325 (1985).
35. Quaranta, N., Gambaro, L., and Thomas, H., *in* "Proceedings of the XII Simposio lberoamericano de Catálisis, Barasil, 1990," Vol. 3, p. 193.
36. Fierro, J. L. G., Gambaro, L. A., Cooper, T. A., and Kremenic, G., *Appl. Catal.* **6**, 363 (1983).
37. Tatibouët, J. M., and Germain, J. E., *C.R. Acad. Sci. Paris* **296**, 613 (1983).
38. Ono, T., Mukai, T., Miyata, H., Ohno, T., and Hatayama, F., *Appl. Catal.* **49**, 273 (1989).